ELSEVIER

Marine Geology 190 (2002) 119–149

MARINE GEOLOGY
INTERNATIONAL JOURNAL OF MARINE GEOLOGY, GEOCHEMISTRY AND GEOPHYSICS

www.elsevier.com/locate/margeo

Last glacial–Holocene paleoceanography of the Black Sea and Marmara Sea: stable isotopic, foraminiferal and coccolith evidence

A.E. Aksu [a,*], R.N. Hiscott [a], M.A. Kaminski [b], P.J. Mudie [c], H. Gillespie [a], T. Abrajano [d], D. Yaşar [e]

[a] *Department of Earth Sciences, Centre for Earth Resources Research, Memorial University of Newfoundland, St. John's, NF, Canada A1B 3X5*

[b] *Department of Geological Sciences, University College London, Gower Street, WC1E 6BT London, UK*

[c] *Geological Survey of Canada–Atlantic, Bedford Institute of Oceanography, 1 Challenger Drive, Dartmouth, NS, Canada B2Y 4A2*

[d] *Department of Earth Sciences, Rensselaer Polytechnic Institute, Rochester, NY, USA*

[e] *Institute of Marine Sciences and Technology, Dokuz Eylül University, Haydar Aliyev Caddesi No. 10, Inciraltı, 35340 Izmir, Turkey*

Received 30 April 2001; accepted 19 February 2002

Abstract

Multi-proxy data and radiocarbon dates from several key cores from the Black Sea and Marmara Sea document a complex paleoceanographic history for the last ~30 000 yr. The Marmara Sea was isolated from both the Black Sea and the Aegean Sea during glacial periods when global sea-level lowering subaerially exposed the shallow sills at the Straits of Bosphorus and Dardanelles (i.e. lake stage), and reconnected through both straits during interglacial periods, when rise of global sea level breached the shallow sills (i.e. gateway stage). Micropaleontological data show that during the 'lake stage' the surface-water masses in both the Marmara Sea and Black Sea became notably brackish; however, during the 'gateway stages' there was a low-salinity surface layer and normal marine water mass beneath. Two sapropel layers are identified in the Marmara Sea cores: sapropels M2 and M1 were deposited between ~29.5 and 23.5 ka, and ~10.5 and 6.0 ka, respectively. Micropaleontological and stable isotopic data show that the surface-water salinities were reduced considerably during the deposition of both sapropel layers M2 and M1, and calculation using planktonic foraminiferal transfer functions shows that sea-surface temperatures were notably lower during these intervals. The presence of fauna and flora with Black Sea affinities and the absence of Mediterranean fauna and flora in sapropels M1 and M2 strongly suggest that communication existed with the Black Sea during these times. A benthic foraminiferal oxygen index shows that the onset of suboxic conditions in the Marmara Sea rapidly followed the establishment of fully marine conditions at ~11–10.5 ka, and are attributed to Black Sea outflow into the Marmara Sea since 10.5 ka. These suboxic conditions have persisted to the present. The data discussed in this paper are completely at odds with the 'Flood Hypothesis' of Ryan et al. (1997), and Ryan and Pitman (1999).

Keywords: Marmara Sea; Black Sea; sapropel; stable isotopes; sea-surface temperature and salinity

* Corresponding author. Tel.: +1-709-737-8385; Fax: +1-709-737-2589.
E-mail address: aaksu@sparky2.esd.mun.ca (A.E. Aksu).

0025-3227/02/$ – see front matter
PII: S0025-3227(02)00345-6

1. Introduction

The Marmara Sea forms a gateway between the world's largest permanently anoxic basin, the Black Sea, and the northeastern extension of the eastern Mediterranean basin, the Aegean Sea (Fig. 1). It is connected to the Black Sea through the Strait of Bosphorus (or Strait of Istanbul; ~40 m deep) and to the Aegean Sea through the Strait of Dardanelles (or Strait of Çanakkale; ~70 m deep). The importance of this gateway has long been recognized in the Quaternary paleoceanographic evolution of the eastern Mediterranean, in particular the development of quasiperiodic sapropel layers (e.g. Olausson, 1961; Vergnaud-Grazzini et al., 1977; Thunell and Williams, 1989; Aksu et al., 1995a,b). Sapropel is defined as a discrete bed, >1 cm thick, which contains greater than 2.0% total organic carbon (TOC) by weight, whereas a sapropelic layer is defined to contain between 0.5 and 2.0% TOC by weight (Kidd et al., 1978). During Quaternary glacial periods, the levels of the Aegean Sea and the Black Sea stood below the sill depths of the Bosphorus and Dardanelles; thus, the Marmara Sea and Black Sea became land-locked basins, isolated from the eastern Mediterranean. During the transition from the last glacial to the Holocene, the eastern European and western Siberian ice sheets began to disintegrate; however, most of the evolving meltwaters drained into the Baltic Sea and North Sea (Prentice et al., 1992). The climate in Europe during the last glacial maximum was notably dryer than today (Peyron et

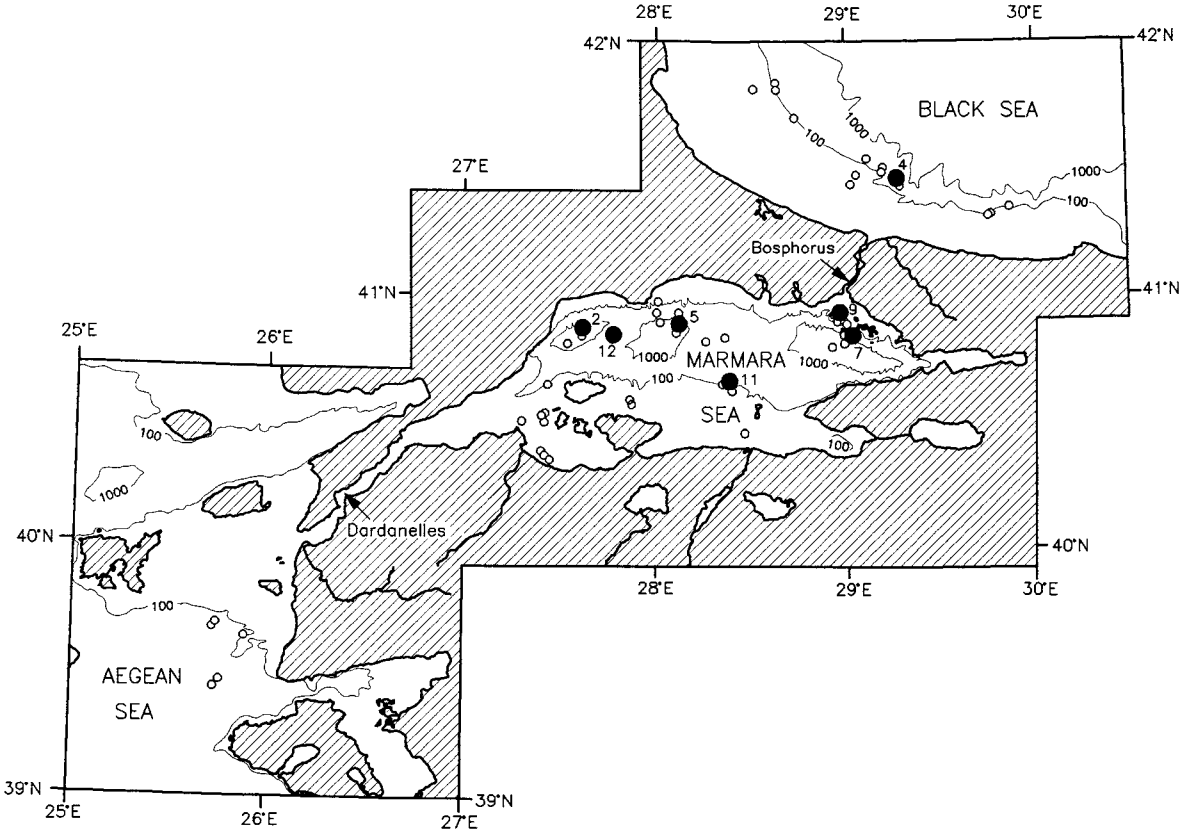

Fig. 1. Location map of the Marmara Sea and the Strait of Bosphorus (=Strait of Istanbul) and Strait of Dardanelles (=Strait of Çanakkale). Circles are gravity cores; large filled circles are key cores discussed in this paper: 4=MAR98-04, 5=MAR94-05, 7=MAR98-07, 9=MAR98-09, 11=MAR97-11 and 12=MAR98-12. Isobaths (100 and 1000) are in metres.

al., 1998; Ramrath et al., 1999), preventing the Black Sea from rising to the Bosphorus sill depth until the Holocene when the climate became progressively more humid so that large rivers draining eastern Europe, such as Danube, Dnieper, Dniester, Bug and Don, raised the level of the Black Sea. Following a rise from a low of ~−110 m at ~11 ka to breach the sill in the Strait of Bosphorus at ~10–10.5 ka (Aksu et al., 2002; Hiscott et al., 2002), the Black Sea began exporting its excess water into the Marmara Sea and the Aegean Sea, creating a low density surface-water layer that contributed to vertical stratification and sapropel deposition (Aksu et al., 1995a,b). This suggestion of an early connection between the Black Sea and Marmara Sea starting at ~10.5 yr BP is supported by a variety of multi-proxy paleoceanographic data that are synthesized in this paper. Detailed palynological data confirming this early connection are presented in Mudie et al. (2002a,b).

2. Present-day physical oceanography

The water exchange between the Black Sea and the eastern Mediterranean Sea occurs through the Straits of Bosphorus and Dardanelles and the intervening Marmara Sea as a two-layer flow (Fig. 2; Latif et al., 1992; Özsoy et al., 1995; Polat and Tuğrul, 1996). The cooler (5–15°C) and lower salinity (17–20‰) surface layer originates from the Black Sea, and flows south/southwest across the straits with velocities of 10–30 cm/s. This water mass forms a 25–100-m-thick surface layer in the Black Sea, the Marmara Sea and in the northeast segment of the Aegean Sea. Warmer (15–20°C) and high-salinity (38–39‰) Mediterranean water flows north along the eastern Aegean Sea. This water mass plunges beneath the low-salinity surface layer in the northeastern Aegean Sea and penetrates the Strait of Dardanelles flowing northeast with velocities of 5–25 cm/s. The Mediterranean water occupies the entire Marmara ba-

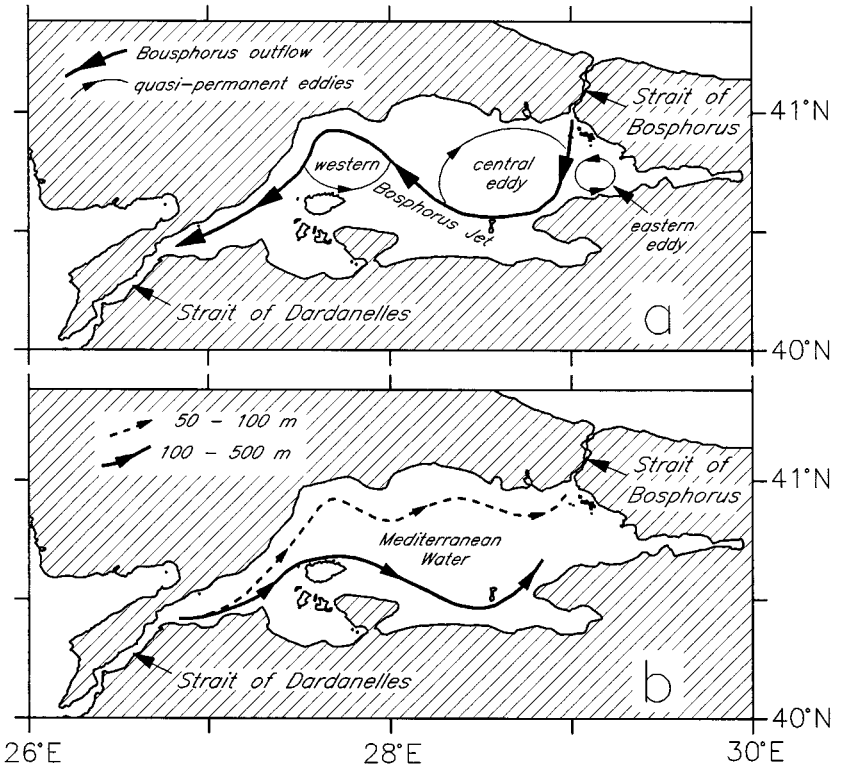

Fig. 2. Surface- (a) and deep- (b) water circulation in the Marmara Sea from Beşiktepe et al. (1994).

sin below a 20–30-m-thick low-salinity surface layer. It travels farther northeast across the Strait of Bosphorus with velocities of 5–15 cm/s, and penetrates the Black Sea where it constitutes the bottom water mass below the 100–200-m-thick surface layer.

Today, there is a net export of ~300 km^3/yr of water from the Black Sea into the Aegean Sea (Özsoy et al., 1995). This outflow results from the excess of precipitation over the Black Sea (~300 km^3/yr) and freshwater input by large rivers (~350 km^3/yr) as compared with evaporation (~350 km^3/yr) over the water body. If the Black Sea did not have an outlet at the Bosphorus, its positive water budget would induce an annual rise of its surface of 94 cm (or 93.7 m/100 yr), assuming a constant surface area. The Danube, Dniester, Dnieper, Southern Bug and Don Rivers drain ~20% of central and eastern Europe (~2 million km^2) and are the major sources of freshwater into the Black Sea (UNESCO, 1969, 1993). Peak river discharges occur during April and May, and the narrow constriction at the Strait of Bosphorus forces the level of the Black Sea to fluctuate ~50 cm in perfect synchronity with the seasonal and interannual discharge variations (Özsoy et al., 1995, 1996). Satellite altimetry shows that the surface of the Black Sea is on average 40 cm above the level of the Marmara Sea which, in turn, is approximately 30 cm above the level of the northern Aegean Sea.

The surface-water circulation in the Black Sea is dominated by two large central cyclonic gyres (eastern and western gyres) and several smaller, anticyclonic coastal eddies (Oğuz et al., 1993). The narrow (<75 km wide) counterclockwise-rotating peripheral 'Rim Current' separates the cyclonic basinal gyres from the anticyclonic coastal eddies (Aksu et al., 2002, their fig. 1). This current flows eastward along the Anatolian coast with velocities of ~20 cm/s and dominates the surface circulation across the narrow continental shelves (Oğuz et al., 1993). The weaker Bosphorus and Sakarya anticyclonic eddies are situated west and east of the Strait of Bosphorus, respectively.

The surface circulation in the Marmara Sea is dominated by the outflow of low-salinity Black Sea water (Beşiktepe et al., 1994). The jet of water entering the Marmara Sea from the Bosphorus flows south-southwest as a narrow current for nearly the entire width of the basin, but curves initially west and later northwest along the southern shelf region (Fig. 2a). This current then crosses the width of the Marmara Sea once more before it swings southwest towards the Strait of Dardanelles, forming large meander loops with three weak anticyclonic gyres (Fig. 2a; Beşiktepe et al., 1994).

The bottom-water circulation in the Marmara Sea is controlled by the rate of influx of denser Mediterranean water through the Strait of Dardanelles. This water mass enters the Marmara Sea, forms turbulent plumes that sink beneath the halocline and slowly travels eastward into the deeper Marmara basins (Fig. 2b).

3. Data acquisition and methods

During the MAR94 (1994), MAR97 (1997), MAR98 (1998) and MAR00 (2000) cruises of the RV *Koca Piri Reis* of the Institute of Marine Sciences and Technology, 65 <2.5-m-long gravity cores (Fig. 1) were collected from the northeastern Aegean Sea, southwestern Black Sea and the Marmara Sea, using a 4-m-long corer with 10-cm internal diameter and 400-kg weight. The core sites were carefully selected using ~7500 line-km of high-resolution Huntec deep-tow boomer/sparker profiles and 40 cubic-inch airgun profiles, located by satellite navigation (GPS).

Cores were stored upright onboard ship and were shipped to Memorial University of Newfoundland (MUN), where they were split, described and photographed. Sediment color was determined using the 'Rock-Color Chart' published by the Geological Society of America in 1984. Seven key cores were identified, in which critical stratigraphic horizons determined in seismic profiles could be studied and dated. These cores were systematically sub-sampled for micropaleontological and stable isotopic studies. Approximately 20 cc sediment was removed at 10-cm intervals from each core. For foraminiferal and coccolith studies, samples were wet-sieved through a 63-μm screen. The coarse fraction was

dried in an oven at 40°C, weighed and dry-sieved through a 125-μm screen. Planktonic foraminifera were identified and counted in each >125-μm fraction using the taxonomic descriptions of Saito et al. (1981) and Kennett and Srinivasan (1983). Benthic foraminifera were identified and counted in four cores, MAR97-11, MAR98-07, MAR98-09 and MAR98-12, following the methods and taxonomy described in Kaminski et al. (2002). For coccolith studies, the <63-μm fractions were wet-sieved through a 20-μm cloth; <2-μm fractions were further separated out using a centrifuge. Coccoliths were identified and counted in the 20–2-μm fractions in all the key cores using the taxonomic descriptions of Kleijne (1993) and Winter et al. (1994). All species counts were converted to percentages.

No one particular benthic or planktonic foraminifera species occurs in sufficient quantities throughout the cores to allow stable isotopic analyzes to be carried out. Therefore, oxygen and carbon isotopes were determined in planktonic foraminifera *Turborotalita quinqueloba* in sections of cores MAR94-05, MAR97-02, MAR97-11, MAR98-09 and MAR98-12 where this species was present, following the methods described in Aksu et al. (1989). In addition, oxygen and carbon isotopes were also determined in benthic foraminifera *Bulimina marginata* in core MAR97-11, *Cassidulina neocarinata* in core MAR98-09 and *Ammonia beccarii* in core MAR98-04. Isotopic measurements were made using a Finnigan MAT 252 triple collector mass spectrometer at MUN. All analyses were run against the internal MUN standard Canada Bay Marble ($\delta^{18}O = -8.58$‰ and $\delta^{13}C = 0.75$‰ versus Pee Dee Belemnite, PDB): the results were subsequently converted to the PDB standard. The analytical precision of the laboratory standards run before and after each analytical session was ±0.03‰, and several duplicate analyses and laboratory standards showed that the reproducibility was better that 0.04‰ for both $\delta^{18}O$ and $\delta^{13}C$.

Forty shell samples were extracted from several levels in 20 cores and were radiocarbon-dated at the IsoTrace Radiocarbon Laboratory of the University of Toronto. In addition, three bivalve carbonate samples were extracted from a single core and radiocarbon-dated at the Beta Analytical Laboratories, FL, USA. A full listing of uncorrected radiocarbon ages and calibrated calendar ages (using a reservoir correction of 415 yr) is presented in Table 1. In this paper, we use only uncalibrated ages with no reservoir correction.

4. Results and interpretation

4.1. Sedimentary data and chronology

The gravity cores in the Black Sea and Marmara Sea were raised from water depths of 30–1207 m. The sedimentary facies correspondingly vary from marginal marine sands and deltaic deposits to hemipelagic muds and organic-rich sapropels in the basins (Abrajano et al., 2002; Hiscott et al., 2002). We use subaerial unconformities and their correlative conformities, as well as flooding surfaces, to subdivide the succession into a number of allostratigraphic units, defined in a companion paper (Hiscott and Aksu, 2002). In both the Black Sea and Marmara Sea, allostratigraphic Unit A extends from the seafloor to a ~11-ka sequence boundary that is an unconformity in modern water depths less than ~100 m, and a correlative conformity elsewhere. In some cores from the Marmara Sea, Unit A is divided into two subunits: A1 (~0–6 ka) and A2 (~6–11 ka; Hiscott and Aksu, 2002). Subunit A2 is a laminated sapropel in deep basins (M1; Abrajano et al., 2002). In both the Black Sea and Marmara Sea allostratigraphic Unit B is only present at water depths greater than ~100 m, and represents basinal or prodeltaic deposition during the ~11-ka lowstand of oxygen isotopic stage 2. In the Marmara Sea, Unit C is a laminated sapropel (M2) like Subunit A2. Cored sediments older than ~30 ka are not divided into allostratigraphic units, but represent a diverse group of older Quaternary deposits cut by the ~11-ka lowstand unconformity: these sediments are not discussed in this paper.

In general, Unit A consists of dark yellowish brown (10YR4/2), olive gray (5Y4/1), brownish gray (5YR4/1), greenish gray (5GY4/1), to moderate olive gray (5Y4/2) bioturbated silty/clayey

Table 1
Radiocarbon ages reported as uncalibrated conventional ^{14}C dates in yr BP (half-life of 5568 yr; errors represents 68.3% confidence limits), and calibrated calender years calculated using OxCal (Stuiver et al., 1998a,b) and a marine reservoir correction of 415 yr (Marine Reservoir Correction Database, Queens University, Belfast, Ireland)

Core # and depth	Latitude	Longitude	Water depth (m)	Dated material	^{14}C date (yr BP)	Calender age (cal BP)	Lab No.[a]
MAR94-05 40 cm	40°52.26′N	28°06.31′E	−850	Foraminifera	21 950 ± 310	N/A	TO-5367
MAR94-05 210 cm	40°52.26′N	28°06.31′E	−850	Foraminifera	29 540 ± 1 540	N/A	TO-5369
MAR97-02 80 cm	40°51.95′N	27°36.84′E	−1080	Bivalve	1 990 ± 50	1 950 ± 110	BE-118903
MAR97-02 150 cm	40°51.95′N	27°36.84′E	−1080	Bivalve	3 810 ± 50	3 755 ± 130	BE-118904
MAR97-02 210 cm	40°51.95′N	27°36.84′E	−1 080	Bivalve	3 490 ± 50	3 370 ± 120	BE-118905
MAR97-11 79 cm	40°39.20′N	28°22.67′E	−111	*Turritella* spp.	10 790 ± 70	12 000 ± 633	TO-7774
MAR97-11 92 cm	40°39.20′N	28°22.67′E	−111	White mussels	12 970 ± 80	14 400 ± 500	TO-7775
MAR97-11 174 cm	40°39.20′N	28°22.67′E	−111	Small oyster	14 940 ± 90	17 400 ± 567	TO-7776
MAR97-11 204 cm	40°39.20′N	28°22.67′E	−111	White mussels	15 590 ± 90	18 150 ± 600	TO-7777
MAR97-12B 47 cm	40°37.51′N	28°23.38′E	−78	*Turritella* spp.	9 920 ± 70	10 950 ± 467	TO-7778
MAR97-15 175 cm	40°31.60′N	27°24.79′E	−65	*Turritella* spp.	9 140 ± 70	10 250 ± 50	TO-9523
MAR97-16 76 cm	40°30.13′N	27°18.63′E	−62	Serpulid bioherm	9 850 ± 70	10 850 ± 467	TO-7779
MAR97-17 175 cm	40°40.25′N	27°25.64′E	−125	White mussel	15 630 ± 100	18 100 ± 650	TO-9524
MAR97-19 179 cm	40°21.27′N	27°26.81′E	−30	*Turritella* spp.	3 890 ± 50	3 860 ± 140	TO-7780
MAR97-20 25 cm	40°22.33′N	27°25.26′E	−32	Serpulid bioherm	6 510 ± 70	6 990 ± 167	TO-8453
MAR97-24 203 cm	40°38.87′N	28°20.95′E	−105	*Turritella* spp.	10 360 ± 80	11 500 ± 567	TO-7781
MAR98-04 24 cm	41°27.26′N	29°16.01′E	−112	*Mytilus*	5 680 ± 60	6 080 ± 125	TO-7782
MAR 98-04 104 cm	41°27.26′N	29°16.01′E	−112	*Mytilus*	5 780 ± 60	6 165 ± 143	TO-7783
MAR98-04 118 cm	41°27.26′N	29°16.01′E	−112	White mussel	33 550 ± 330	N/A	TO-7784
MAR98-07 72 cm	40°50.98′N	29°00.98′E	−95	White mussel	15 210 ± 100	17 650 ± 600	TO-7785
MAR98-07 95 cm	40°50.98′N	29°00.98′E	−95	*Dreissena r. distincta*	43 550 ± 790	N/A	TO-8455
MAR98-07 119 cm	40°50.98′N	29°00.98′E	−95	White mussel	41 480 ± 610	N/A	TO-7786
MAR98-07 180 cm	40°50.98′N	29°00.98′E	−95	White mussel	41 900 ± 610	N/A	TO-7787
MAR98-07 217 cm	40°50.98′N	29°00.98′E	−95	White mussel	40 460 ± 590	N/A	TO-7788
MAR98-09 35 cm	40°55.36′N	28°56.80′E	−64	*Anomia* spp.	4 500 ± 60	4 650 ± 145	TO-7789
MAR98-09 42 cm	40°55.36′N	28°56.80′E	−64	*Nuclea nucleus*	6 120 ± 70	6 540 ± 160	TO-8455
MAR98-09 52 cm	40°55.36′N	28°56.80′E	−64	*Varicorbula gibba*	8 810 ± 100	9 400 ± 333	TO-8456
MAR98-09 60 cm	40°55.36′N	28°56.80′E	−64	*Turritella* spp.	9 070 ± 70	9 700 ± 433	TO-7790
MAR98-09 94 cm	40°55.36′N	28°56.80′E	−64	*Turritella* spp.	9 840 ± 80	10 850 ± 467	TO-7791
MAR98-09 113 cm	40°55.36′N	28°56.80′E	−64	*Mytilus* spp.	10 220 ± 70	11 200 ± 500	TO-7792
MAR98-12 50 cm	40°50.54′N	27°47.68′E	−549	Bivalve fragment	4 200 ± 100	4 300 ± 300	TO-8457
MAR98-12 130 cm	40°50.54′N	27°47.68′E	−549	*Nuculacea* spp.	10 660 ± 130	11 850 ± 667	TO-8458
MAR98-16 23 cm	39°40.76′N	25°44.19′E	−126	*Turritella* spp.	9 630 ± 70	10 400 ± 500	TO-7793
MAR00-05 60 cm	41°49.01′N	28°30.68′E	−83	*Mytilus* spp.	5 460 ± 70	5 850 ± 167	TO-9137
MAR00-05 167 cm	41°49.01′N	28°30.68′E	−83	*Cardium* spp.	6 600 ± 60	7 090 ± 140	TO-9088
MAR00-06 45 cm	41°50.38′N	28°37.54′E	−127	*Mytilus* spp.	2 160 ± 60	2 370 ± 0	TO-9138
MAR00-06 124 cm	41°50.38′N	28°37.54′E	−127	*Mytilus* spp.	7 770 ± 70	8 200 ± 147	TO-9089
MAR00-08 54 cm	41°42.16′N	28°43.32′E	−96	*Mytilus* spp.	5 780 ± 70	6 165 ± 157	TO-9139
MAR00-08 116 cm	41°42.16′N	28°43.32′E	−96	*Mytilus* spp.	6 590 ± 70	7 070 ± 167	TO-9090
MAR00-09 119 cm	41°42.38′N	29°06.31′E	−115	*Mytilus* spp.	5 740 ± 60	6 132 ± 139	TO-9525
MAR00-13 95 cm	40°56.05′N	28°55.78′E	−84	*Abra* spp.	8 030 ± 70	8 575 ± 217	TO-9110
MAR00-13 217 cm	40°56.05′N	28°55.78′E	−84	Varicorbula gibba	9 170 ± 80	9 800 ± 500	TO-9111
MAR00-23 170 cm	41°19.82′N	29°45.53′E	−98	*Mytilus* spp.	6 760 ± 60	7 295 ± 115	TO-9526

[a] IsoTrace Radiocarbon Laboratory, Accelerator Mass Spectrometry Facility, University of Toronto. Errors attached to the calibrated calender years represent 95% confidence limits, but do not account for analytical errors of the ^{14}C dates.

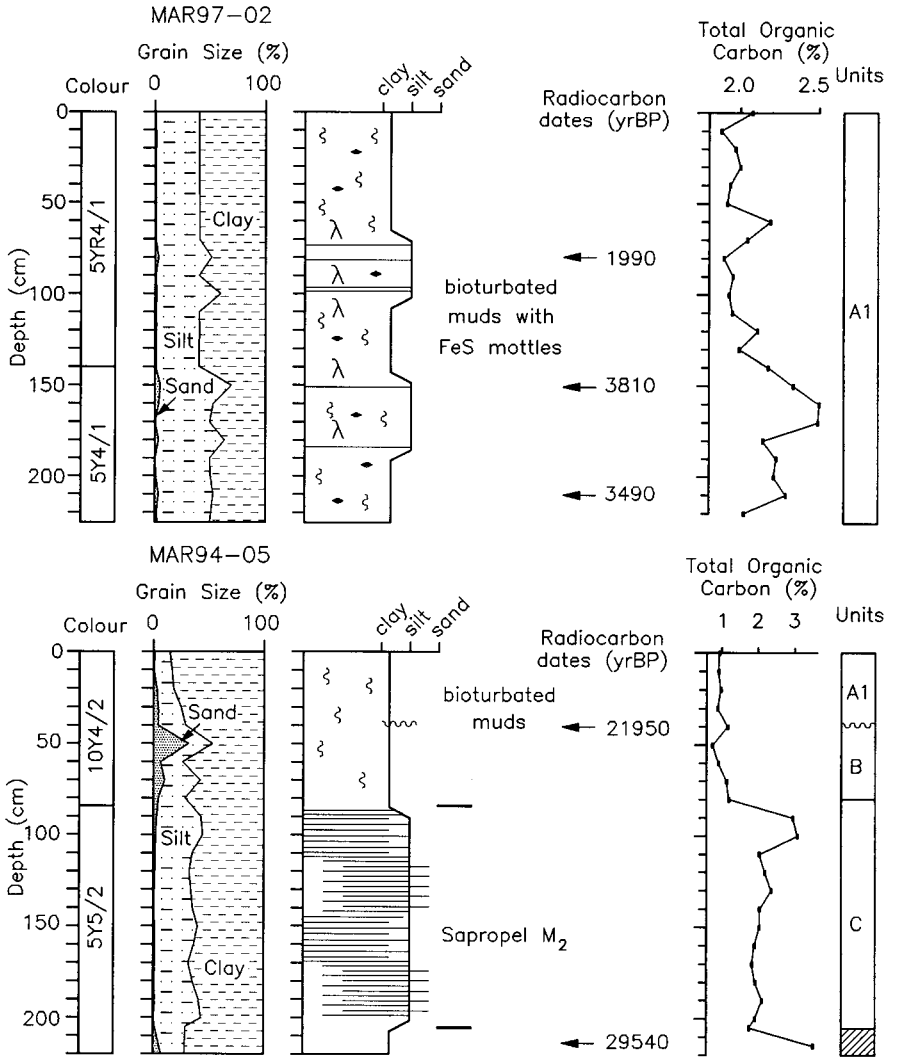

Fig. 3. Summary of allostratigraphy, grains size, TOC and radiocarbon ages in cores MAR97-02 and MAR94-05. See Fig. 1 for locations.

muds. The sand fraction is almost entirely biogenic, consisting of foraminifera, gastropods and bivalves, whereas the silt–clay fraction contains notable quantities of coccoliths in the Black Sea core MAR98-04, as well as the basinal Marmara Sea cores MAR97-02 and MAR98-12 (Figs. 3, 4 and 6). TOC values are moderate to high in Subunit A1, ranging from 0.9 to 2.0% in basinal Marmara Sea cores MAR97-02 and MAR98-12, and from 1.0 to 1.5% in the shelf cores MAR97-11 and MAR98-09 (Figs. 3–5; Abrajano et al., 2002).

At shelf depths, Subunit A2 consists of olive gray (5Y3/2) to grayish olive (10Y4/2) silty/clayey muds with noticeably fewer microfossils in all grain-size fractions than Subunit A1, moderate burrow density, and low TOC content. Subunit A2 in the deep basinal cores from the Marmara Sea is much darker (olive black, 5Y2/1), unburrowed and displays distinctive faint parallel lamination/bedding which is commonly associated with color banding. The TOC values in these basinal cores (e.g. MAR98-12) are generally above

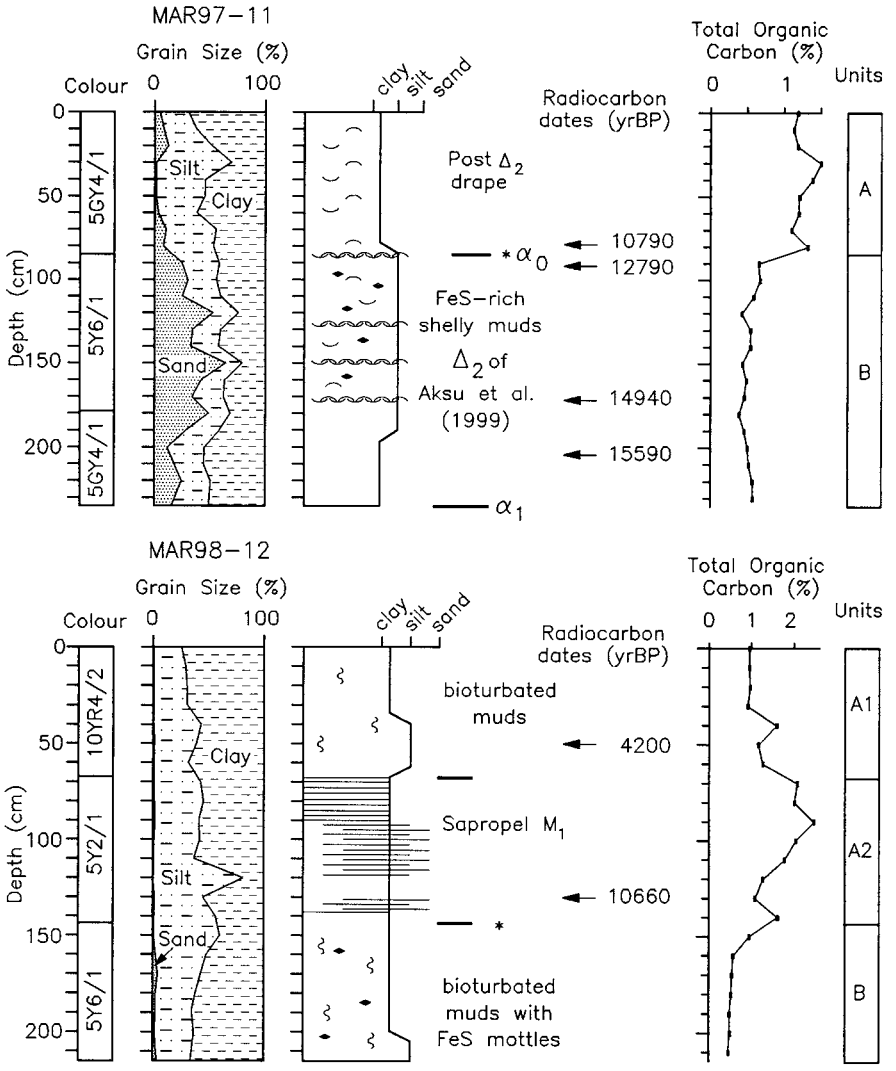

Fig. 4. Summary of allostratigraphy, grains size, TOC and radiocarbon ages in cores MAR97-11 and MAR98-12. See Fig. 1 for locations.

2.0%, exceeding 2.4% in the upper portion of Subunit A2 (Abrajano et al., 2002), including very high concentrations of pollen and terrestrial spores (Mudie et al., 2002b). The sand fraction is mostly calcareous biogenic remains. There are abundant Fe-monosulfide mottles and minor pyritized or pyrite-filled microfossils. Radiocarbon dates (Table 1) show that this subunit spans ~10.5–6 ka and broadly correlates in age with sapropel S1 of the Aegean Sea (Aksu et al., 1995a,b).

Unit B consists of dark greenish gray (5GY4/1) to light olive gray (5Y6/1) silty muds (Figs. 3–6). TOC values are consistently low in Unit B, ranging from 0.3 to 0.6% (Figs. 3–5; Abrajano et al., 2002). The unit contains very low planktonic foraminifera and coccolith abundances, low dinoflagellate concentrations (Mudie et al., 2002a), but high benthic foraminifera and gastropod abundances (MacDonald, 2000; Kaminski et al., 2002).

Unit C was recovered in only a few cores col-

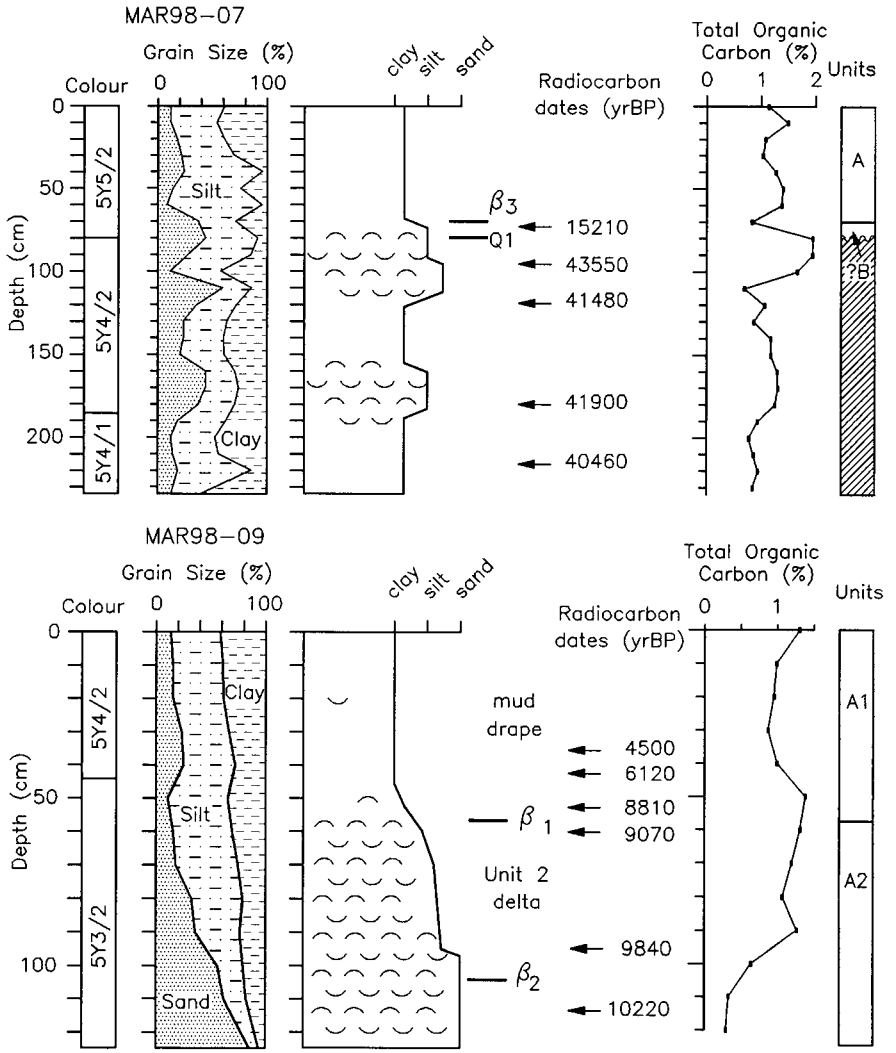

Fig. 5. Summary of allostratigraphy, grains size, TOC and radiocarbon ages in cores MAR98-07 and MAR98-09. See Fig. 1 for locations.

lected from the base of the northern slope of the central and western basins in the Marmara Sea (e.g. core MAR94-05; Fig. 3). It consists of olive black (5Y2/1) unborrowed silty muds with distinct parallel laminations associated with color banding. In core MAR94-05, the transition between Subunit A1 and Unit B is a disconformity. There is a sharp downcore increase in TOC values from ~1.0% in Unit B to ~3.0% in Unit C (Fig. 4; Abrajano et al., 2002). The TOC values remain consistently high (2.0–3.5%) throughout Unit C (Fig. 4). Rare sand consists mainly of foraminifera tests. Diatoms are abundant.

All sediments recovered from the Marmara Sea as well as Subunits A1 and A2 in the Black Sea can be classified as sapropelic deposits; however, Subunit A2 and Unit C in the basinal Marmara Sea cores MAR98-12 and MAR94-05, respectively, represent true sapropel layers. There are numerous discrete sapropel deposits in the Qua-

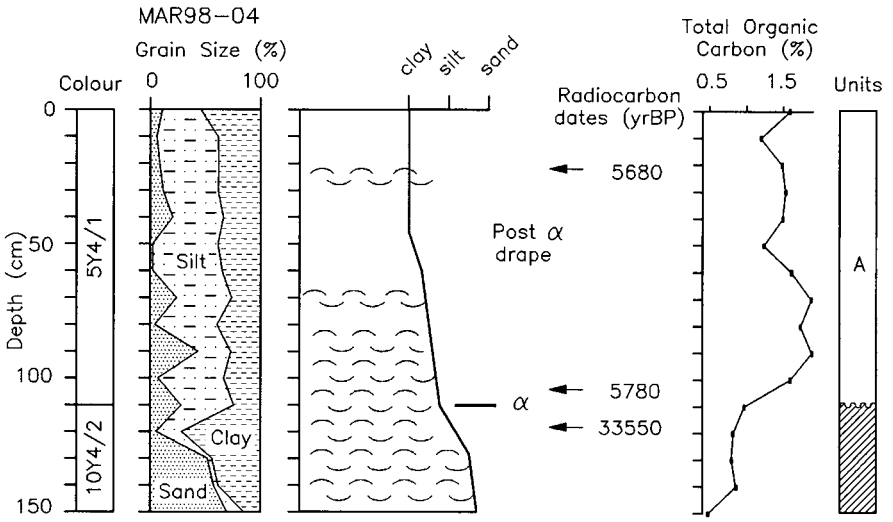

Fig. 6. Summary of allostratigraphy, grains size, TOC and radiocarbon ages in core MAR98-04. See Fig. 1 for location.

ternary sediments of the eastern Mediterranean Sea, including the Aegean Sea. These are labelled from youngest to the oldest as S1, S2, S3, etc. (Vergnaud-Grazzini et al., 1977; Rossignol-Strick, 1985). To avoid confusion, the sapropel layers in the Marmara Sea cores are denoted as M1 (Subunit A2) and M2 (Unit C).

4.2. Calcium carbonate preservation

All cores contain scattered to abundant bivalves and gastropods, including well-preserved transparent shells of planktonic pteropods (MacDonald, 2000). A clear decline is observed in the percentage of well-preserved transparent shells, and a reciprocal increase in specimens with opaque-white shells with increasing depth in cores MAR97-11, MAR98-04 and MAR98-09. This transition is ascribed to a deterioration of aragonite preservation of the pteropod shells with depth (Almogi-Labin et al., 1986).

Aragonite has a much higher solubility in marine waters than calcite (e.g. Berger, 1977); therefore, the occurrence of pteropods in nearly every sample studied from the Marmara and Black Sea cores implies excellent preservation of the less labile calcitic skeletons which form the planktonic and benthic foraminiferal and coccolith assemblages.

4.3. Planktonic foraminifera

Planktonic foraminifera are entirely absent in Black Sea cores (e.g. MAR98-04), but are abundant in Marmara Sea cores where the fauna displays a low species diversity, overwhelmingly dominated by *Turborotalita quinqueloba* with variable but smaller numbers of *Globigerina bulloides* and *Neogloboquadrina pachyderma* dextral, and minor occurrences of *Globigerinoides ruber*, *Globigerinoides sacculifer*, *Globigerinita uvula*, and *N. pachyderma* sinistral (Figs. 7–9). This planktonic foraminiferal assemblage, dominated by the North Atlantic subpolar species *T. quinqueloba*, *G. bulloides*, and *N. pachyderma* dextral, reflects the present-day temperature and salinity conditions of the Marmara Sea. These species are also reported in the cooler regions of the Mediterranean Sea, such as the northern Aegean Sea (Thunell, 1978; Aksu et al., 1995b), where winter surface temperatures vary between 10°C and 16°C (Aksu et al., 1995b). Here, we report the occurrence of this fauna in the marginal Marmara Sea, where winter temperatures range between 5°C and 10°C, with corresponding very low salinities of 20–21‰. The planktonic foraminiferal fauna of the northern Aegean Sea surface sediments is dominated by the subtropical species *G. ruber* and to a lesser extent *G. sacculifer*. In the Mar-

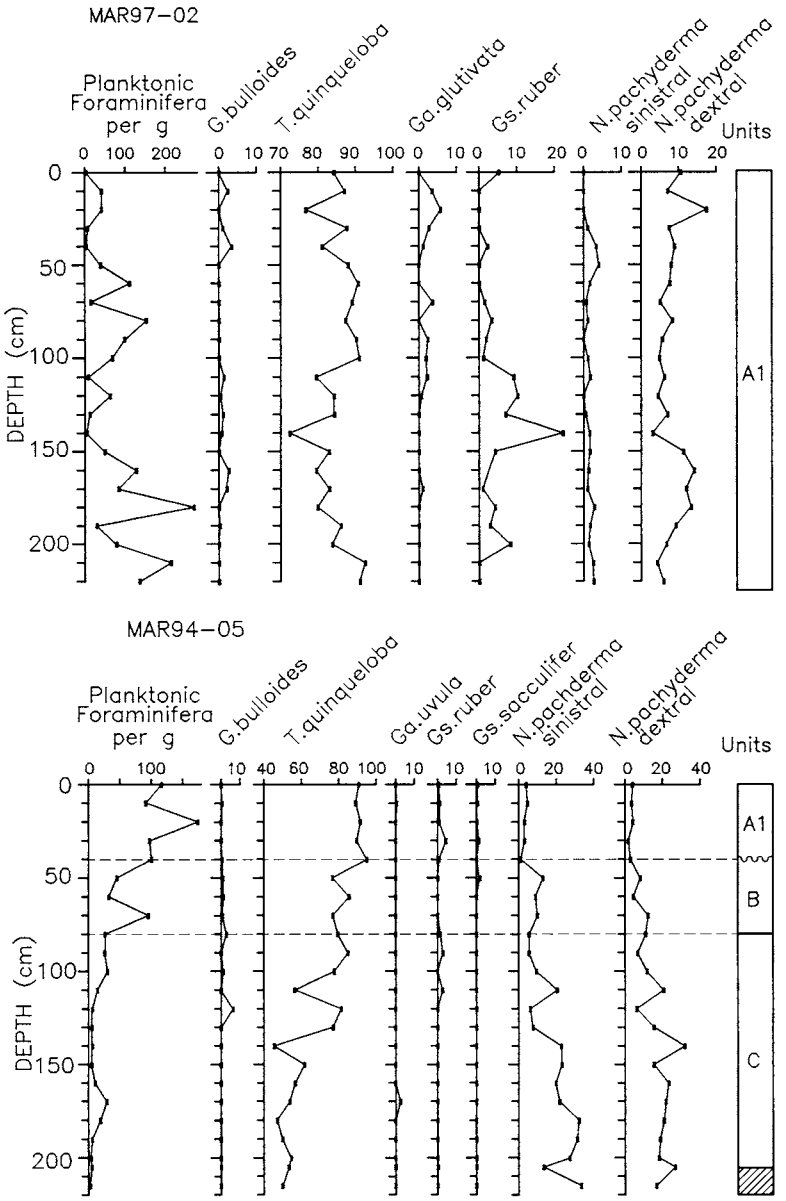

Fig. 7. Planktonic foraminiferal assemblages in cores MAR97-02 and MAR94-05. Total planktonic foraminiferal abundance is presented as specimens per gram dry weight sediment; species frequencies are in percent of total. Allostratigraphic units are defined by Hiscott and Aksu (2002). See Fig. 1 for locations.

mara Sea cores, these same subtropical species show a reciprocal relationship with the subpolar species, suggesting that intervals containing notable quantities of the subtropical species probably reflect stronger northward penetration of Mediterranean water masses into the Marmara Sea.

Subunit A1 in the Marmara Sea cores is characterized by high planktonic foraminiferal abundance, comparable to core tops in northern Aegean Sea cores (Aksu et al., 1995b). The fauna is generally dominated by *Turborotalita quinqueloba*, *Globigerina bulloides*, and *Neogloboquadrina pa-*

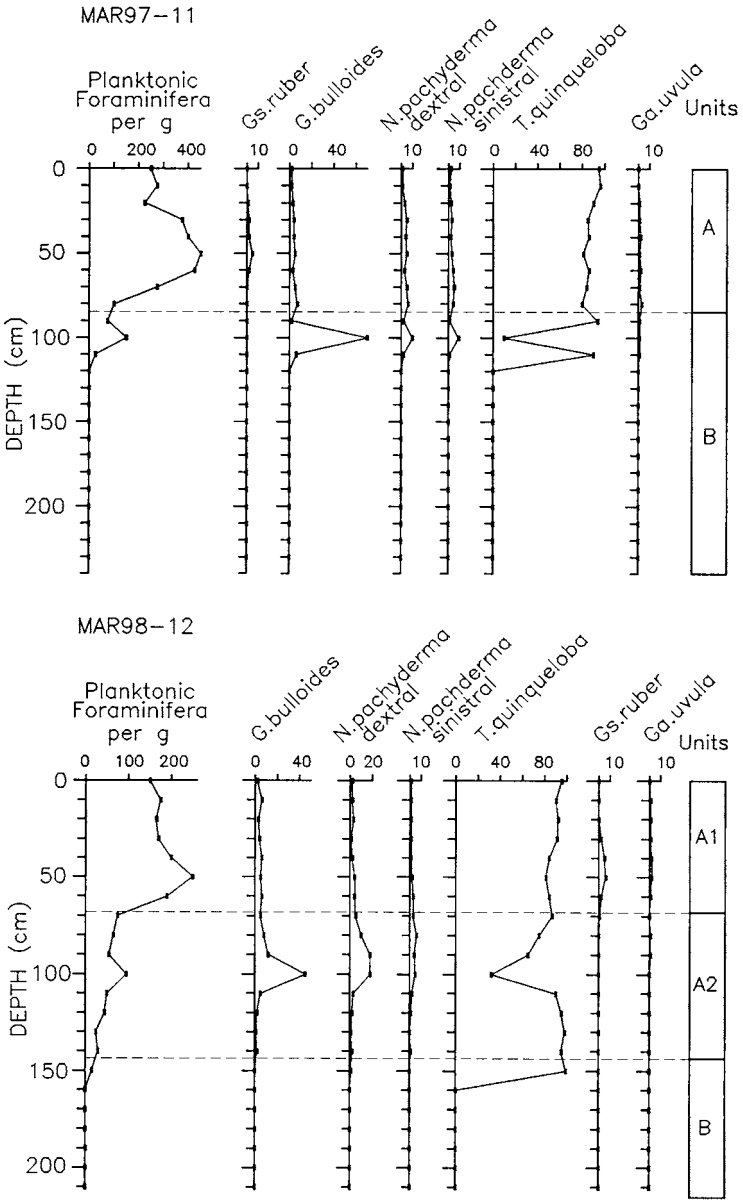

Fig. 8. Planktonic foraminiferal assemblages in cores MAR97-11 and MAR98-12. Total planktonic foraminiferal abundance is presented as specimens per gram dry weight sediment; species frequencies are in percent of total. Allostratigraphic units are defined by Hiscott and Aksu (2002). See Fig. 1 for locations.

chyderma dextral; however, the lower portion of Subunit A1 in cores MAR97-02, MAR98-09 and MAR98-12 also contains 10–20% *Globigerinoides ruber* and minor occurrences of *Globigerinoides sacculifer* (Figs. 7–9). The Subunit A1–A2 transition is marked by a sharp decrease in total planktonic foraminifera in the cores studied, associated with a gradual change in faunal assemblage (Figs. 8 and 9). Subunit A2 displays a notable downcore decline in total planktonic foraminiferal abundances. The faunal assemblage of Subunit A2 in the basinal core MAR98-12, and to a lesser

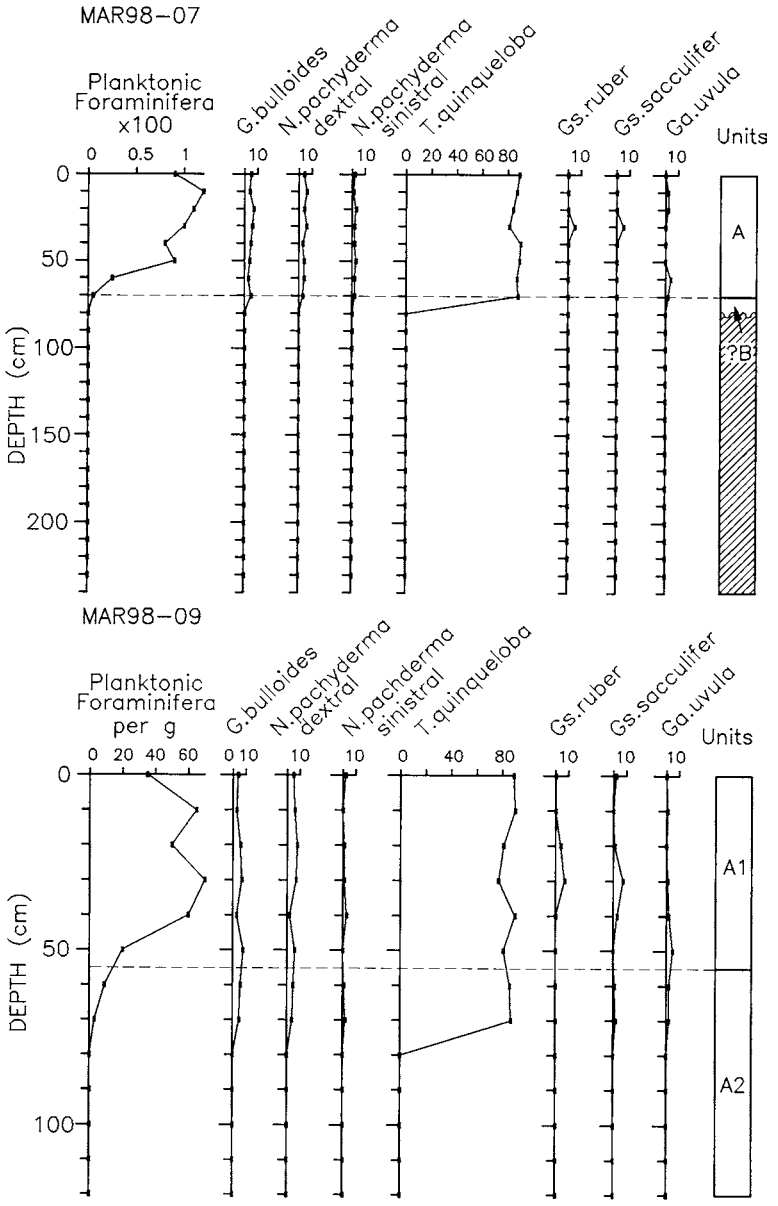

Fig. 9. Planktonic foraminiferal assemblages in cores MAR98-07 and MAR98-09. Total planktonic foraminiferal abundance is presented as specimens per gram dry weight sediment; species frequencies are in percent of total. Allostratigraphic units are defined by Hiscott and Aksu (2002). See Fig. 1 for locations.

extent shelf cores MAR97-11 and MAR98-09, is still dominated by *T. quinqueloba*, but relative to Subunit A1 it contains significantly higher percentages of polar species *N. pachyderma* sinistral as well as subpolar species *G. bulloides* and *N. pachyderma* dextral (Figs. 8 and 9). The lower portion of Subunit A2 in core MAR98-09 is barren of planktonic foraminifera (Fig. 9).

Unit B is barren of planktonic foraminifera in Marmara Sea cores MAR97-11 and MAR98-12, but contains a low-diversity, low-abundance assemblage in core MAR94-05, where the fauna is

dominated by polar and subpolar species *Turborotalita quinqueloba*, *Globigerina bulloides*, and *Neogloboquadrina pachyderma* sinistral and dextral (Figs. 7–9). Unit C is characterized by very low planktonic foraminiferal abundances, marked by a notable increase in polar species *N. pachyderma* sinistral, as well as subpolar species *N. pachyderma* dextral, associated with a reciprocal decrease in *T. quinqueloba* (Fig. 7).

4.4. Coccoliths

Coccolith assemblages in the Marmara Sea and Black Sea cores exhibit a low diversity and abundance, overwhelmingly dominated by *Emiliania huxleyi* with variable but significant occurrences of *Helicopondosphaera wallichii*, *Helicopondosphaera selli* and *Helicopondosphaera kemptaneri*, and minor occurrences of *Syracosphaera pulchra*, *Braarudosphaera bigelowii*, *Calcidiscus leptoporus*, *Gephyrocapsa oceanica*, *Rhobdosphaera clavigera*, *Umbilicosphaera tenuis*, *Helicosphaera carteri* and *Reticulofenestra* species (Figs. 10–13). This floral assemblage is similar to those described from northern Aegean Sea cores (Aksu et al., 1995b), as well as eastern Mediterranean Sea cores (Erba et al., 1987; Raffi et al., 1993; Castradori, 1993). The dominance of *E. huxleyi* in Black Sea cores has previously been reported (Bukry, 1974).

Coccoliths are relatively abundant in the Black Sea core MAR98-04. The upper portion of Unit A includes a high-abundance, low-diversity flora, dominated by *Emiliania huxleyi* with minor occurrences of *Braarudosphaera bigelowii*, *Helicopondosphaera* species, and *Discolithina* species (Fig. 10). The lower portion of Unit A displays a sharp decrease in total coccolith abundances and the disappearance of Quaternary coccoliths. Instead, the flora in here includes isolated occurrences of reworked coccoliths of mainly Eocene age, including *Coccolithus eopelagicus* and *Coccolithus pseudogammation* (Fig. 10). The lowermost portion of Unit A is barren of coccoliths. Older sediments below the shelf crossing unconformity, α (Aksu et al., 2002), show an increase in coccolith abundances where the flora is dominated by pre-Quaternary *Reticulofenestra* species. The absence of true oceanic coccoliths in the Black Sea sediments such as *Calcidiscus leptoporus*, *Gephyrocapsa oceanica*, *Rhobdosphaera clavigera*, *Umbilicosphaera*

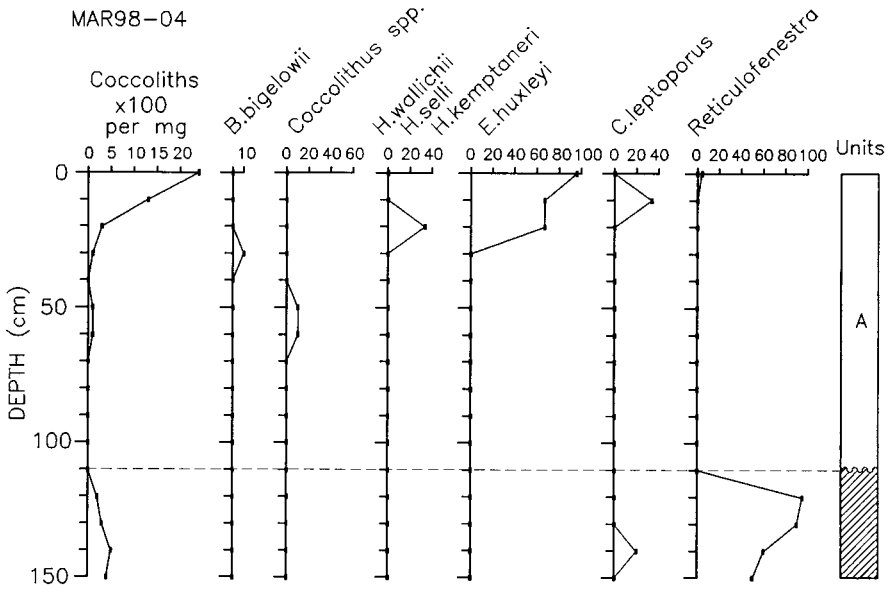

Fig. 10. Coccolith assemblages in core MAR98-04. Total coccolith abundance is presented as specimens per milligram dry weight sediment; species frequencies are in percent of total. Allostratigraphic units are defined by Hiscott and Aksu (2002). See Fig. 1 for location.

tenuis and *Helicosphaera carteri* is notable, and probably reflects salinities below the tolerance of most *Coccolithophyceae* (Winter et al., 1994).

Coccolith abundances in the Marmara Sea cores (Figs. 11–13) are comparable to those observed in eastern Black Sea cores (Bukry, 1974) and northern Aegean Sea cores (Aksu et al., 1995b). Unit A is characterized by a high-abundance, high-diversity flora dominated by *Emiliania huxleyi* (Figs. 11–13). However, unlike the Black Sea, the flora in the Marmara Sea cores contains small but significant quantities of oceanic coccoliths, including *Coccolithus pelagicus*, *Calcidiscus leptoporus*, *Gephyrocapsa oceanica*, *Rhabdosphaera clavigera*, *R. pulchra*, *R. sessilis*, *Umbilicosphaera tenuis*, and *Helicosphaera carteri* (Figs. 11–13). The downcore transition from Subunit A1 to A2 is characterized by a notable decline in

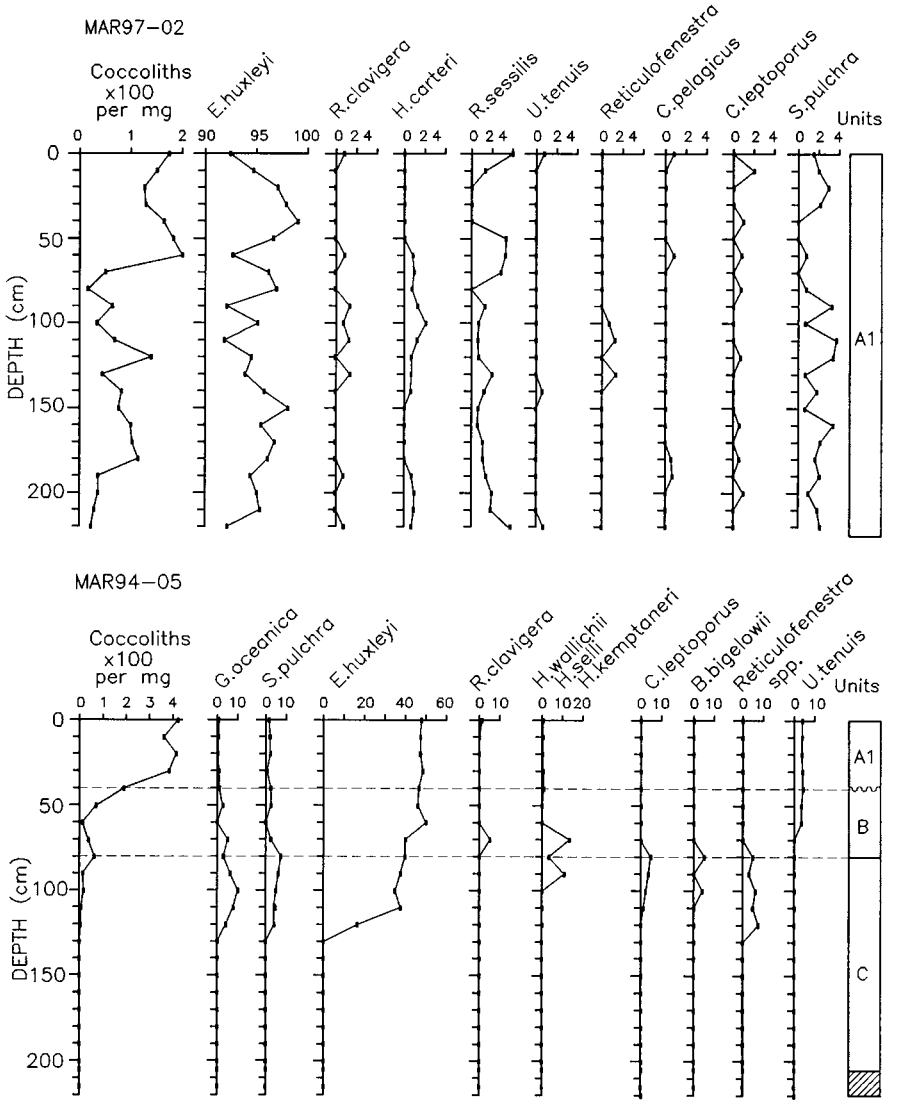

Fig. 11. Coccolith assemblages in cores MAR97-02 and MAR94-04. Total coccolith abundance is presented as specimens per milligram dry weight sediment; species frequencies are in percent of total. Allostratigraphic units are defined by Hiscott and Aksu (2002). See Fig. 1 for locations.

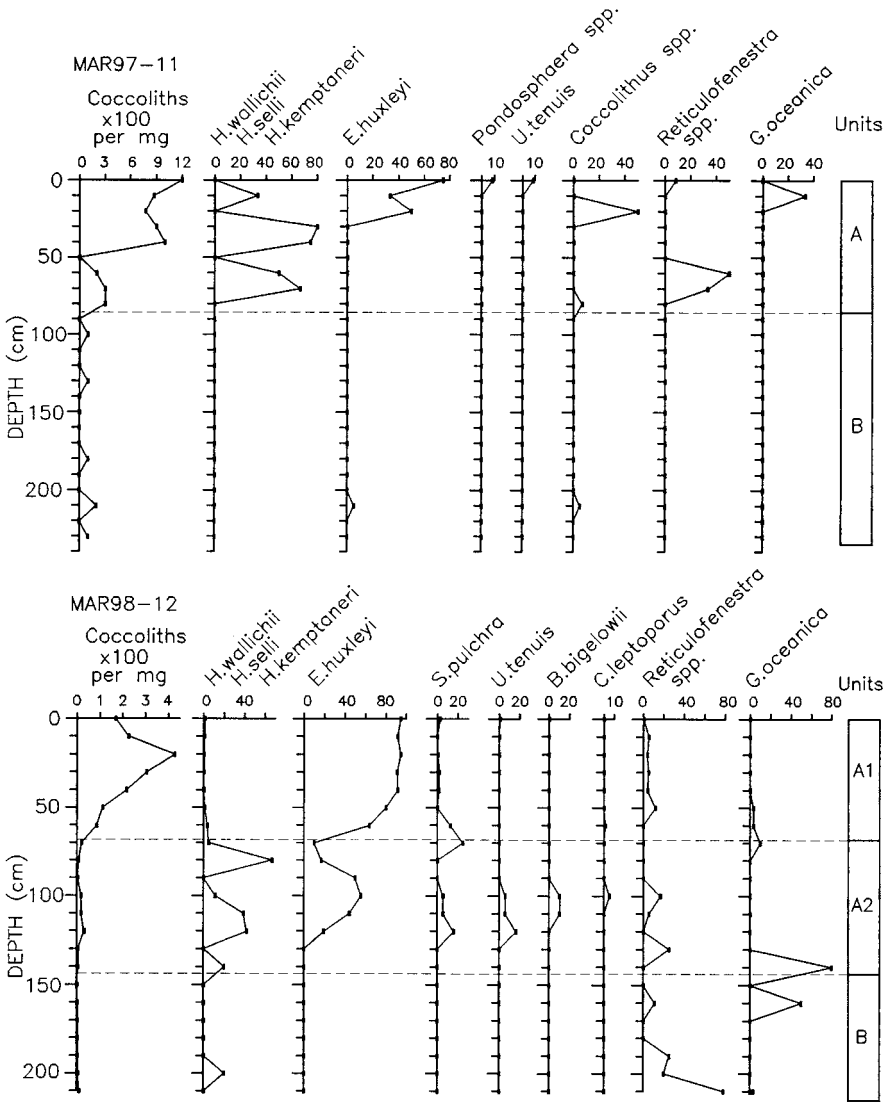

Fig. 12. Coccolith assemblages in cores MAR97-11 and MAR98-12. Total coccolith abundance is presented as specimens per milligram dry weight sediment; species frequencies are in percent of total. Allostratigraphic units are defined by Hiscott and Aksu (2002). See Fig. 1 for locations.

coccolith abundances, associated with a subtle floral change (Fig. 12). For example, Subunit A2 in Marmara Sea basinal core MAR98-12 displays a low-abundance and low-diversity floral assemblage co-dominated by *E. huxleyi* and *Helicopondosphaera* species, mainly *Helicopondosphaera wallichii*, *Helicopondosphaera selli* and *Helicopondosphaera kemptaneri*. The base of this unit is marked by a major spike of *G. oceanica* (Fig. 12). Distribution patterns of living coccolithophores in the Mediterranean Sea show that highest frequencies of *G. oceanica* and small gephyrocapsids occur in regions of salinity minima (37.0–37.5‰), with values 1.5–2.0‰ lower than normal salinity values of the eastern Mediterranean surface water (Knappertsbusch, 1993). The spike of *G. oceanica* at the base of Subunit A2 in the basinal Marmara Sea core possibly indicates reduction of surface-

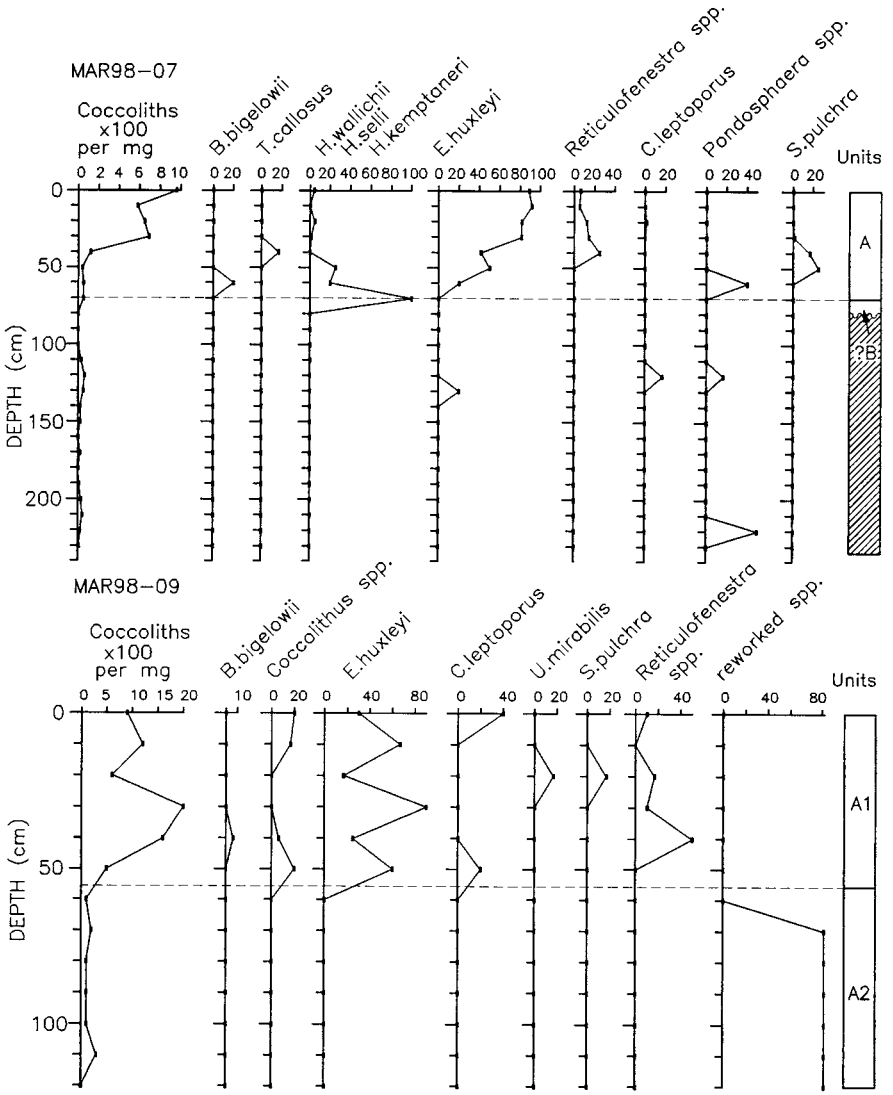

Fig. 13. Coccolith assemblages in cores MAR98-07 and MAR98-09. Total coccolith abundance is presented as specimens per milligram dry weight sediment; species frequencies are in percent of total. Allostratigraphic units are defined by Hiscott and Aksu (2002). See Fig. 1 for locations.

water salinities. Similar significant occurrences of *Gephyrocapsa* species, particularly *G. oceanica*, *G. aperta* and *G. muellerae*, are also observed in the Aegean Sea sapropel S1 (Aksu et al., 1995a,b). Unit B in the Marmara Sea cores either contains very low abundances or is barren of coccoliths (Figs. 11–13). Coccoliths are only present in the uppermost portion of Unit C, whereas the lower part of this unit is barren of coccoliths (Fig. 11).

4.5. Benthic foraminiferal morphogroups

The occurrence and distribution of benthic foraminifera in the Marmara Sea cores are discussed by Kaminski et al. (2002). Here, only the benthic foraminiferal morphogroups and their paleoceanographic implications are considered. Benthic foraminiferal assemblage data from cores MAR97-11, MAR98-07, MAR98-09 and MAR98-

12 were used to calculate the benthic foraminiferal oxygen index (BFOI) of Kaiho (1991). The benthic foraminiferal assemblages in the cores did not include any significant amount of organically cemented agglutinated taxa; therefore, the BFOI was calculated using the calcareous forms. In modern oceans, this index displays a linear relationship with the oxygen content of bottom waters, at least in the range of values below 3 ml/l (Kaiho, 1994). Recent CTD data collected from the central Marmara Sea reveal that dissolved oxygen values in the surface mixed layer of the water column are ~5 ml/l (Institute of Marine Sciences and Technology database, unpublished). The values begin to decline just below the halocline at a water depth of ~20 m, and by −35 m reach dissolved oxygen values below 2 ml/l. Below this depth the dissolved oxygen content of the water declines slowly, and by −100 m depth values are in the suboxic range, i.e. below 1.5 ml/l. The dissolved oxygen content beneath the halocline is below 2% throughout the Marmara Sea. The relative proportions of three benthic foraminiferal morphogroups are used to provide an estimate of the dissolved oxygen content of the bottom waters. Kaiho (1991) adapted the morphogroup concepts of Bernhard (1986) and Corliss and Chen (1988) to define these three groups. 'Dysoxic' species have flattened, tapered, or elongate tests which typically display a thin, porous wall and lack ornamentation. The genera *Bolivina*, *Brizalina*, *Cassidulina*, *Chilostomella*, *Fursenkoina* and *Globobulimina* are placed into this group. Numerous studies have documented the occurrence of these genera in dysoxic environments worldwide (Corliss and Chen, 1988; Kaiho, 1991). 'Oxic' species display a variety of test forms, including spherical, planoconvex, biconvex, and rounded trochospiral. This group includes species that have large, ornamented tests and thick walls. The genera *Agglutinella*, *Ammonia*, *Anomalinoides*, *Asterigerinata*, *Cibicides*, *Globocassidulina*, *Gavelinopsis*, *Planorbulina*, *Rosalina*, and *Valvulineria*, as well as all the lagenids and miliolids are included in this group. Finally, the 'intermediate' or 'suboxic' group contains taxa that are typically larger than the 'dysoxic' forms, and may display some ornamentation. This group includes tapered and cylindrical forms such as *Amphicorina*, *Angulogerina*, some *Bulimina*, *Uvigerina*, textulariid genera, the planispiral forms such as *Haynesina*, *Nonionella*, *Melonis*, elphidiid genera, and those trochospiral forms that have small, thin test walls such as *Aubignyna* and *Gyroidinoides*. Most of these genera live infaunally under conditions of normal oxygenation, but live closer to the sediment–water interface in dysoxic environments (Kaminski et al., 2002).

The deepest locality studied for benthic foraminifera is core MAR98-12, recovered from a present-day water depth of 549 m. Samples from the basal section of the core are barren of foraminifera (Fig. 14). At 130 cm, just above the base of sapropel M1 (~10 660 yr BP; Fig. 4), a bloom of *Fursenkoina* is observed accompanied by a few specimens of *Brizalina* and *Bulimina* (Kaminski et al., 2002). The entry of these marine species points to establishment of a marine connection between the Marmara Sea and the Aegean Sea. However, the lack of any species belonging to the 'aerobic' or 'intermediate' morphogroups indicates that the deeper waters of the Marmara Sea were severely dysoxic, with dissolved oxygen concentrations probably below 0.5%. Samples collected from the sapropel layer M1 itself are also barren of foraminifera, or contain just a few specimens of *Chilostomella*, *Bolivina*, and *Brizalina* which may have been downmixed by burrowers. The paucity of benthic foraminifera, and the rare and sporadic occurrences of dysoxic species suggest that conditions during the deposition of the sapropel must have been close to anoxic. Near the top of the sapropel layer at 90 cm, a bloom in *Globobulimina* is observed, indicating a slight improvement in bottom-water oxygenation. At 80 cm, miliolids and *Hyalina* appear, while *Uvigerina* makes an appearance at 20 cm. The dominance of the 'dysoxic' morphogroup throughout the core and the absence of aerobic forms within sapropel M1 suggests dysoxic to suboxic conditions (below 1.5%) since ~10.5 ka.

Core MAR97-11, at ~111 m water depth, is well-suited to study the Holocene history of oxygenation at intermediate depths in the water column. The sparse benthic foraminiferal assemblages recovered from the base of core MAR97-11

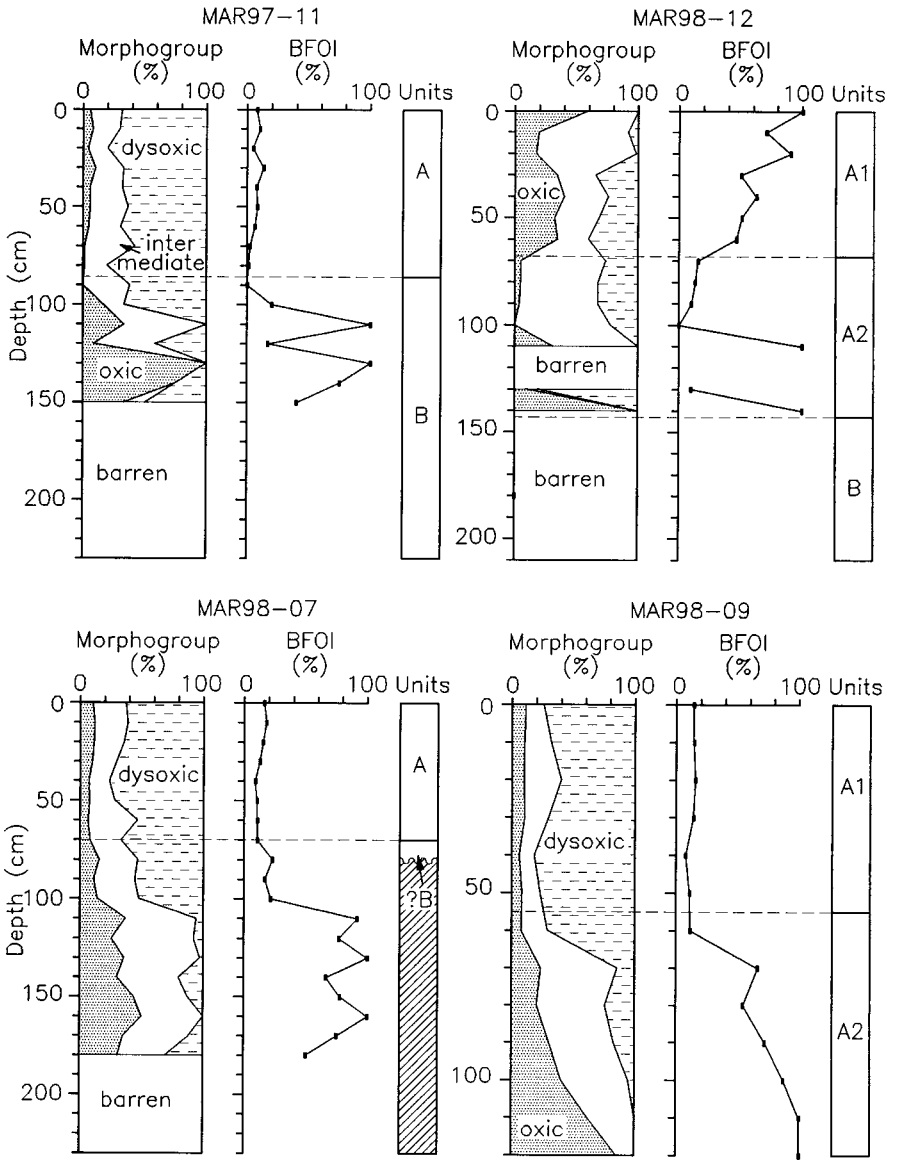

Fig. 14. Abundance of dysoxic, intermediate and oxic assemblages and BFOI in cores MAR97-11, MAR98-07, MAR98-09 and MAR98-12. Allostratigraphic units are defined by Hiscott and Aksu (2002).

reveal BFOI values that are variable, but generally high (Fig. 14). It is likely that these assemblages contain specimens reworked from older (glacial age) sediments that were deposited under well-oxygenated conditions. Between 70 and 90 cm, the assemblage is dominated by *Fursenkoina* and *Cassidulina* (Kaminski et al., 2002) and registers BFOI values between 0 and 3. These low values point to a dissolved oxygen content below 1.5% suggesting that after ~12 ka the sub-halocline waters of the Marmara Sea became rapidly suboxic. From this minimum, the BFOI values increase slightly upcore.

The sparse benthic foraminiferal assemblages recovered from the base of core MAR98-07 also reveal high BFOI values. Between 110 and 100 cm,

a permanent shift is observed toward low BFOI values (Fig. 14). However, the assemblages at this level are very sparse and may be a result of mixing by burrowers. At the base of the marine drape (Hiscott and Aksu, 2002) at 65 cm in core MAR98-07, the abundant foraminiferal assemblages have BFOI values near 10, which correspond to a dissolved oxygen content of ~1.5%. The BFOI values in MAR98-07 never reached zero, and show that although the bathymetric difference between cores MAR97-11 (−111 m) and MAR98-07 (−95 m) is only 16 m,

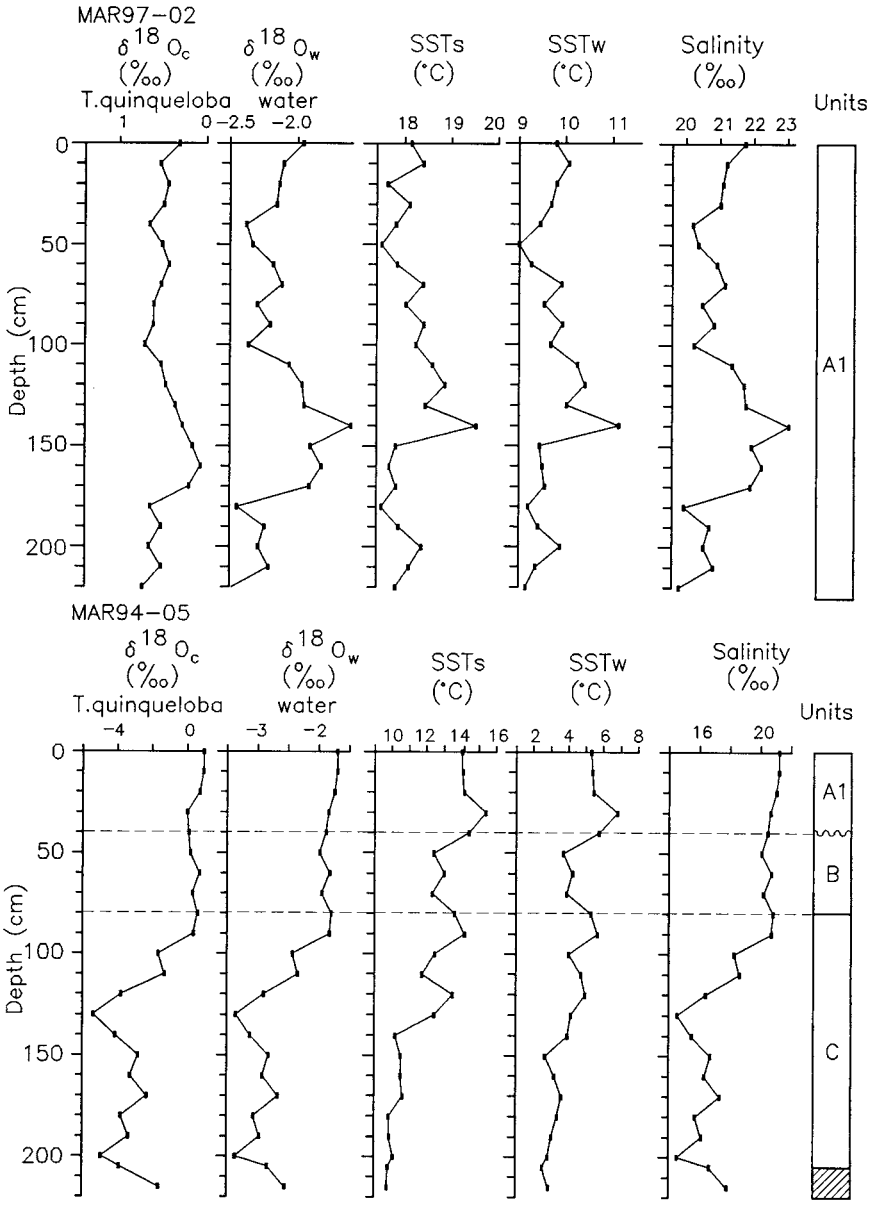

Fig. 15. Oxygen isotopic composition of planktonic foraminifera *Turborotalita quinqueloba*, estimates of oxygen isotopic composition of surface water, SST estimates and sea-surface salinity estimates in cores MAR97-02 and MAR94-05. Allostratigraphic units are defined by Hiscott and Aksu (2002).

the BFOI values are slightly higher at the shallower locality.

MAR98-09 at water of −64 m is the shallowest core studied in detail for benthic foraminifera. The deltaic interval near the base of the core (Hiscott et al., 2002) is dominated by the 'oxic' morphogroup (Fig. 14). The 'dysoxic' forms are entirely absent at 120–110 cm, but first appear in small numbers at 100 cm depth in the core. Their relative proportion increases steadily upcore, becoming dominant at 60 cm. This change reflects the drowning of the delta as sea level rose, and

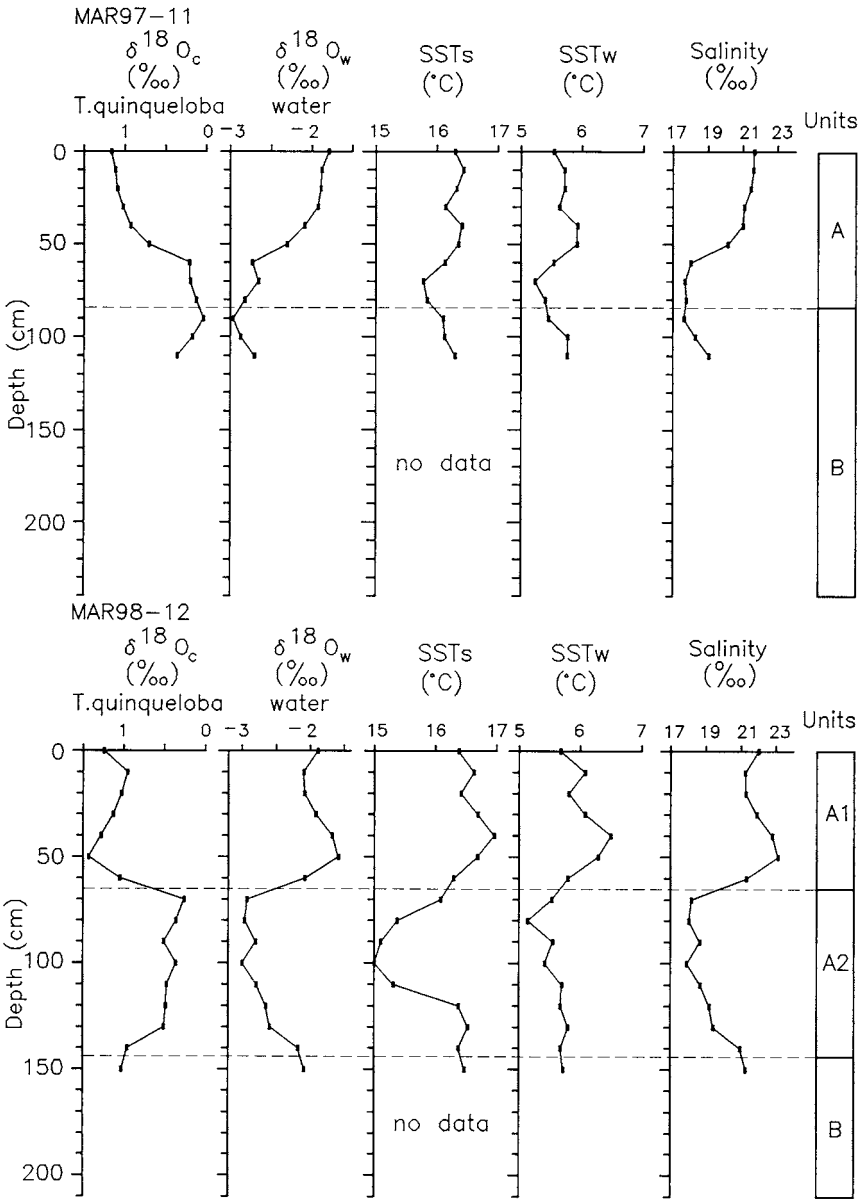

Fig. 16. Oxygen isotopic composition of planktonic foraminifera *Turborotalita quinqueloba*, estimates of oxygen isotopic composition of surface water, SST estimates and sea-surface salinity estimates in cores MAR97-11 and MAR98-12. Allostratigraphic units are defined by Hiscott and Aksu (2002).

the onset of stratification of the water column when the 'dysoxic' forms become dominant at the site at ~9 ka. The BFOI values within the marine mud drape of Subunit A1 stabilize at close to 15, suggesting an oxygen concentration between 1.5 and 2.0% (Fig. 14). A small rise in the BFOI values is observed upcore within the marine drape. The calculated BFOI values for the benthic foraminiferal morphogroups in the core-top sample are in remarkable agreement with the measured dissolved oxygen content of 1.71% at same depth in the central Marmara Sea (IMST database, unpublished), confirming the validity of the BFOI method in this area.

4.6. $\delta^{18}O$ in foraminifera

The $\delta^{18}O$ records of planktonic foraminifera *Turborotalita quinqueloba* in all cores from the Marmara Sea display relatively heavy values in the upper part of Unit A, ranging from 0.0 to 1.5‰ (Figs. 15–17). Core MAR97-02 contains the most expanded record of Subunit A1 with fluctuations ranging between 0.0 and 1.0‰ (Fig. 15). In cores MAR98-09 and MAR98-12, the transition from Subunit A1 to Subunit A2 is marked by a 0.5–1.0‰ depletion in $\delta^{18}O$ values and, in three cores which penetrate Subunit A2, this interval is marked by notably depleted $\delta^{18}O$ values ranging from 0.0 to 0.5‰ (Figs. 15–17). The $\delta^{18}O$ values in Unit B range from 0.0 to 0.5‰ in core MAR94-05, similar to those in the overlying Subunit A1 (Fig. 15): Unit B is largely barren of planktonic foraminifera in cores MAR97-11 and MAR98-12. In core MAR94-05, Unit C displays an approximately 4.0‰ depletion downcore from the overlying Unit B (Fig. 15). Although there are ~1.0‰ fluctuations, the $\delta^{18}O$ values within Unit C consistently remain light.

The $\delta^{18}O$ and $\delta^{13}C$ records in various benthic foraminiferal species are more complete, extending to the base of Marmara Sea cores MAR97-11 and MAR98-09 (Fig. 18). Benthic foraminifera provide the only isotopic record from the southwestern Black Sea in core MAR98-04 (Fig. 18). The $\delta^{18}O$ of *Neocarinata crassa* in core MAR98-09 displays constant values across Subunit A1 and

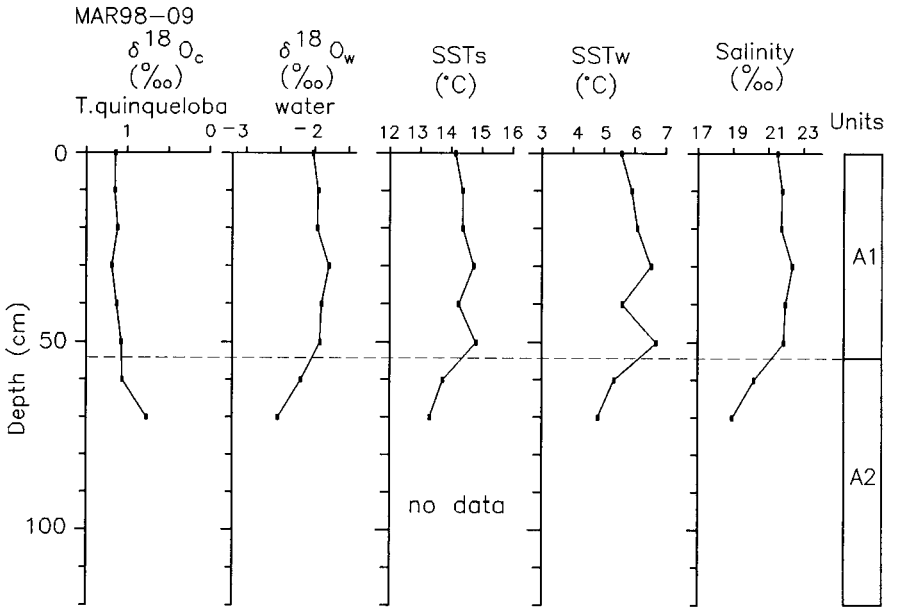

Fig. 17. Oxygen isotopic composition of planktonic foraminifera *Turborotalita quinqueloba*, estimates of oxygen isotopic composition of surface water, SST estimates and sea-surface salinity estimates in core MAR98-09. Allostratigraphic units are defined by Hiscott and Aksu (2002).

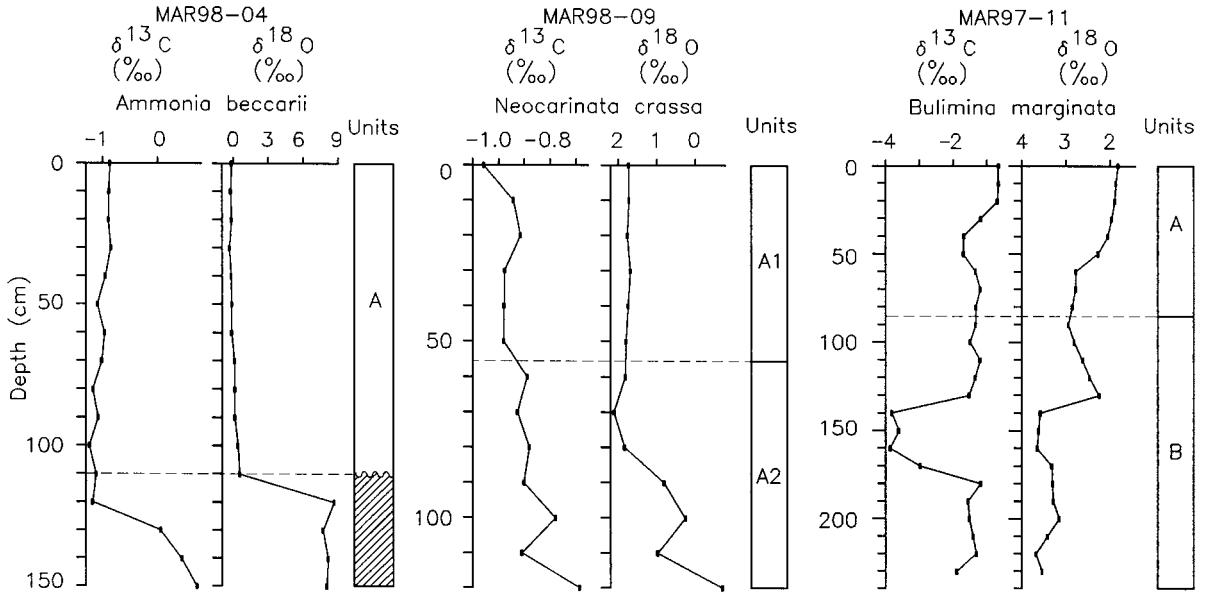

Fig. 18. Oxygen isotopic composition of benthic foraminifera *Ammonia beccarii* in Black Sea core MAR98-04, and *Neocarinata crassa* and *Bulimina marginata* in Marmara Sea cores MAR98-09 and MAR97-11, respectively. Allostratigraphic units are defined by Hiscott and Aksu (2002).

the upper portion of Subunit A2, below which there is a steady depletion across the lower portion of Subunit A2 (Fig. 18). The downcore variations in $\delta^{13}C$ in this core display a reciprocal relationship to the $\delta^{18}O$ variations, increasing from $\sim -1.0‰$ in Subunit A1 to $\sim -0.7‰$ in the lower portion of Subunit A2 (Fig. 18). The oxygen isotopic record of *Bulimina marginata* in core MAR97-11 shows constant $\delta^{18}O$ values in Unit A and the upper portion of Unit B, with a $\sim 1.0–1.5‰$ enrichment at ~ 140 cm depth in the core and fluctuating $\delta^{18}O$ values across the lower portion of Unit B. The carbon isotopic composition in *B. marginata* in this core shows a near reciprocal downcore variation to that observed in the oxygen isotopic record, with enriched carbon isotopic values in Unit A and the upper portion of Unit B, and a notable $\sim 2.0‰$ depletion at ~ 140 cm depth in the core, where the $\delta^{18}O$ record shows $\sim 1.0–1.5‰$ enrichment (Fig. 18). In the lower portion of Unit B, the oxygen and carbon isotopic records lose their reciprocal relationship, in that the $\delta^{13}C$ record displays a progressive $\sim 2.0‰$ enrichment between 150 and 180 cm depth, but the $\delta^{18}O$ values remain unchanged (Fig. 18).

The oxygen isotopic record of *Ammonia beccarii* in the Black Sea core MAR98-04 shows constant $\delta^{18}O$ and $\delta^{13}C$ values in Unit A; however, a remarkable enrichment of 8.5–9.0‰ in $\delta^{18}O$ and $\sim 2.0‰$ in $\delta^{13}C$ is observed at the transition to the underlying older deposits beneath the shelf crossing unconformity, α (Fig. 18).

The oxygen and carbon isotopic records of cores from the Marmara Sea and Black Sea are unlike those from the open ocean. In open ocean sediments, depleted and enriched oxygen isotopic intervals correspond to interglacial and glacial periods, respectively (e.g. Vergnaud-Grazzini et al., 1977). Instead, the observed oxygen isotopic variations in the Marmara Sea and Black Sea cores display a nearly reciprocal relationship with the open ocean record, so that interglacial and glacial intervals are represented by heavy and light $\delta^{18}O$ values, respectively. These variations must have been controlled by local salinity variations, which appear to have been much greater than those developed during the interglacial–glacial cycles of

the Quaternary in the open ocean. Local salinity variations in the Marmara Sea and Black Sea are, in turn, controlled by freshwater input into the Black Sea (glacial meltwater and/or river water) and the degree of communication of the Marmara Sea and Black Sea with the Aegean Sea via the Straits of Bosphorus and Dardanelles.

4.7. Sea-surface temperature (SST) variations

Downcore SST estimates for the Marmara Sea were made using a transfer function. Pseudo-factor matrices were constructed using the planktonic foraminiferal assemblage data from the Marmara Sea and the varimax description matrix of Thunell (1979) followed by application of his transfer function. Winter SST estimates for the core tops range from 5.5°C in the northeastern core MAR98-09 to 9.9°C in the westernmost core MAR97-02, whereas the summer SST estimates vary from 14.1°C in core MAR98-09 to 18.1°C in core MAR97-02 (Figs. 15–17). These core-top values are remarkably similar to the actual winter and summer SSTs from the Marmara Sea (Institute of Marine Sciences and Technology database, unpublished). Nevertheless, our analysis depends on downcore trends in SST values and not their precise magnitudes.

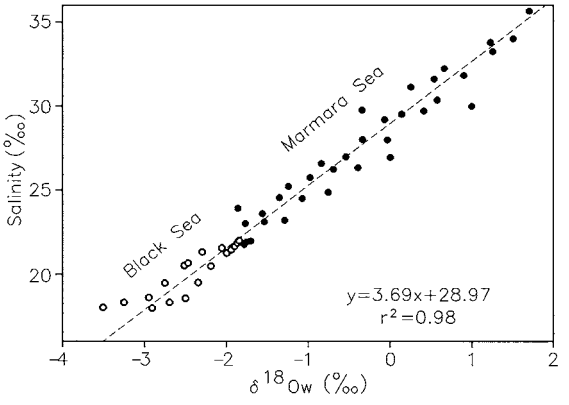

Fig. 19. Relationship between the salinity (Institute of Marine Sciences and Technology database, unpublished) and the oxygen isotopic composition of the water masses in the Marmara Sea (filled circles) and the Black Sea (open circles). Data from Rank et al. (1999).

The SST values in Subunit A1 show little downcore variation, except in the high sedimentation rate core MAR97-02 (Fig. 15). The transition from Subunits A1 to A2 is marked by a sharp decrease in both winter and summer SST estimates in all cores studied (Figs. 16 and 17). In both cores MAR97-11 and MAR98-12, Subunit A2 is characterized by a 1.5°C cooling in the summer SST values, associated with a smaller (~0.5°C) decrease in the winter SST values (Fig. 16). The Subunit A1–A2 transition in MAR98-09 shows a similar, but more pronounced downcore decrease of approximately 2°C in both summer and winter SST estimates (Fig. 17).

In core MAR94-05, the SST estimates for Unit B range from 4.0 to 5.0°C and 12.5 to 13.0°C for winter and summer, respectively, then decline to ~3°C and ~10°C in Unit C at 215 cm near the base of the core (Fig. 15).

4.8. Sea-surface salinity variations

Sea-surface salinity variations were estimated using the technique described by Aksu et al. (1995a). Briefly, the technique involves (i) the determination of the $\delta^{18}O$ of the surface waters ($\delta^{18}O_w$) using the paleotemperature equation of Shackleton (1974), where the Mediterranean-based planktonic foraminiferal transfer function provides the SSTs needed in this equation, and (ii) the determination of salinity estimates using a regression equation that relates the present-day $\delta^{18}O_w$ values and the surface-water salinities in the Black Sea and Marmara Sea (Fig. 19). Actual measurements of $\delta^{18}O_w$ from the Black Sea and Marmara Sea have been published by Rank et al. (1999). Modern salinity data were obtained from the archive of the Institute of Marine Sciences and Technology, which includes an extensive data set of various CTD (conductivity, depth, temperature) profiles collected from both the Black Sea and the Marmara Sea in close proximity of the stations sampled by Rank et al. (1999). The $\delta^{18}O_w$ versus salinity plot shows a strong positive relationship between these variables, with a correlation coefficient $r^2 = 0.98$ (Fig. 19).

The oxygen isotopic composition of surface waters ($\delta^{18}O_w$) is estimated using the following

paleotemperature equation of Shackleton (1974), which relates the oxygen isotopic composition of foraminiferal calcite ($\delta^{18}O_c$) to the oxygen isotopic composition of the sea water ($\delta^{18}O_w$), provided that an accurate SST estimate can be made:

$$T = 16.9 - 4.38(\delta^{18}O_c - \delta^{18}O_w) + 0.10(\delta^{18}O_c - \delta^{18}O_w)^2 \quad (1)$$

T is the temperature of surface sea water and is calculated using the Mediterranean-based planktonic foraminiferal transfer function of Thunell (1979). In Eq. 1, only the $\delta^{18}O$ values of planktonic foraminifera *Turborotalita quinqueloba* are used as $\delta^{18}O_c$. This species deposits its shell out of isotopic equilibrium, with an average vital effect of 1.3‰ for $\delta^{18}O$ (Volkman and Mensch, 2001). The calculated $\delta^{18}O_w$ values are corrected using this vital effect and the results show that $\delta^{18}O_w$ values in the Marmara Sea oscillated between −1.5‰ and −3.5‰ (Figs. 15–17).

The $\delta^{18}O_w$ estimates in cores MAR97-11, MAR98-09 and MAR98-12 are relatively constant at ∼−1.9‰ to −2.2‰ across the upper part of Unit A (either undifferentiated as in MAR97-11, or as Subunit A1), but show ∼0.4–1.3‰ depletion at the downcore transition into the lower part of Unit A or into Subunit A2 (Figs. 15–17). The $\delta^{18}O_w$ estimates remain noticeably depleted throughout the lower portion of Unit A in core MAR97-11 and Subunit A2 in MAR98-12 (Fig. 16). In core MAR94-05, the $\delta^{18}O_w$ estimates are constant at ∼−2.0‰ across Subunits A1 and Unit B, but show a 1.0–1.5‰ depletion across the Unit B–C transition, and consistent low values in Unit C remain depleted, ranging between −3.5‰ and −2.5‰ (Fig. 15).

An internally consistent picture emerges from trends in the sea-surface salinity estimates in Marmara Sea cores MAR94-05, MAR97-02, MAR97-11, MAR98-09 and MAR98-12, even if individual estimates include some uncertainty. The salinity values in Unit A range between 21.0‰ and 22.5‰, with core-top values remarkably consistent with the present-day salinity measurements in the Marmara Sea (Figs. 15–17). The surface-water salinity estimates show a 2.0–3.0‰ decrease across the Subunit A1–A2 transition, and the salinity estimates remain consistently low in the lower portion of Unit A (e.g. MAR97-11) and Subunit A2 (e.g. MAR98-12). Salinity estimates for Unit B are constant at ∼21‰, but show a much larger decrease across the downcore transition into Unit C, where salinity estimates fluctuate between 15‰ and 17‰ (Fig. 15).

5. Discussion

In recent years, there has been a renewed interest in the paleoceanographic history of the Black Sea and Marmara Sea, particularly the events that took place during the last glacial to Holocene transition. For example, based on data from the northern Black Sea shelf, Ryan et al. (1997) and Ryan and Pitman (1999) suggested that the Black Sea became a giant freshwater lake during the last glacial maximum, with the water level standing at −150 m, and that during the post-glacial sea-level rise at ∼7150 yr BP the Mediterranean Sea breached the Strait of Bosphorus, catastrophically re-filling the Black Sea basin and contributing to the Noah's Flood myth (Mestel, 1997). A number of related papers have been published since, in both the scientific literature as well as popular magazines and books (e.g. Ryan and Pitman, 1999) discussing the effects and implications of this perceived catastrophic oceanographic event. This hypothesis was contradicted by Aksu et al. (1999), who suggested that it was instead the Black Sea that first breached the Bosphorus and overflowed into the Marmara Sea. Hiscott et al. (2002) present additional data that solidify the conclusion that the Black Sea first breached the Bosphorus at ∼10.5 ka. The Ryan et al. (1997) and Ryan and Pitman (1999) hypothesis is also contradicted by multi-proxy climatic and oceanographic data from Aegean Sea cores which show that the last glacial–Holocene transition in the Aegean Sea was accompanied by a ∼10°C increase in SST and 1.0–1.5‰ decrease in sea-surface salinity (Aksu et al., 1995a,b). Aksu and coworkers argued that the depressed salinities in the Aegean Sea required strong Black Sea outflow

between 9.6 and 6.4 ka to form a low-salinity surface lid, which prevented vertical mixing and ventilation, thus promoting the deposition of sapropel S1 in the Aegean Sea (Aksu et al. 1995a,b). The essentially time-equivalent sapropel M1 in the Marmara Sea records the same outflow event. Other workers have confirmed the findings of Aksu et al. (1995a,b) and indicate that the Marmara Sea sapropel (M1) was deposited during a time of increased supply of terrestrial organic carbon, including pollen, fern spores, and fungal remains (Mudie et al., 2002b), associated with high freshwater input from the Black Sea (Çağatay et al., 1999, 2000; Görür et al., 2001).

Multi-proxy data from several dated cores document a complex paleoceanographic history for the last ~30 000 yr, involving the isolation of the Black Sea and the Marmara Sea from the Aegean Sea during glacial periods when low global sea level subaerially exposed the shallow sills in the Straits of Bosphorus and Dardanelles, and the reconnection of these inland seas with the eastern Mediterranean Sea during interglacial periods, when rising global sea level breached the shallow sills. Below we step sequentially through the late Quaternary history of the gateway area.

5.1. Middle Weichselian interval

A reconstructed sea-level curve valid for Mediterranean localities (Skene et al., 1998), as well as the sea-level curve of Chappell and Shackleton (1986) show that during the middle Weichselian Pleniglacial (interstadial), equivalent to oxygen isotopic stage 3 (e.g. Imbrie et al., 1984), sea level stood above the sill depth of the Strait of Dardanelles, at ~−46 m elevation by ~30 ka. Radiometric dates on raised beaches around the western Marmara Sea document an average of 0.45 mm/yr uplift of the western Marmara region, including the Strait of Dardanelles (Yaltırak et al., 2002). Therefore, the floor of the Strait of Dardanelles at ~30 ka was approximately 13.5 m deeper, or at an elevation of −83.5 m assuming constant rates of uplift. During this time, the Marmara Sea must have been fully connected to the Aegean Sea. A number of delta packages (Δ_3, Δ_4, and Δ_5 of Aksu et al., 1999) which developed between ~65 and 25 ka landward of the present-day 75-m isobath along the southern Marmara shelf require that the sea level during isotopic stage 3 was higher than the breach depth of the Strait of Dardanelles. The postulated sea level in the Marmara Sea at ~30 ka is about 5 m below the sill depth of the Strait of Bosphorus. The low-salinity estimates in core MAR94-05 suggest that the level of the Black Sea must have been at or above the breach depth of Bosphorus and that Black Sea must have been connected to the Marmara via a south flowing river.

The micropaleontological and stable isotopic data from core MAR94-05 and dinoflagellate assemblages in this core (Mudie et al., 2001) clearly show that surface-water salinities were reduced considerably during the deposition of sapropel M2 (Unit C), from ~23.5 to 29.5 ka. How could the surface salinities in the Marmara Sea decrease while it remained connected to the Aegean Sea? The middle Weichselian Pleniglacial (oxygen isotopic stage 3) was a period of increased pluviality in the eastern Mediterranean, as indicated by the development of many large inland lakes in Turkey (Roberts, 1983), and enlargement and deepening of existing lakes (e.g. Ramrath et al., 1999). This interval was also characterized by permafrost degradation and climatic warming in northwestern Europe, associated with increased fluvial discharges (e.g. Huijzer and Vandenberghe, 1998). This period must have been accompanied by a noticeable increase in the discharges of rivers flowing into the Black Sea. It is postulated that the freshening of the surface waters in the Marmara Sea was largely due to enhanced precipitation over the eastern Mediterranean region, thus enhancing freshwater outflow from the Black Sea into the Marmara Sea through a river located in the vicinity of the modern Strait of Bosphorus. By implication, the level of the Black Sea must have been high at this time (Çağatay et al., 1999, 2000; Görür et al., 2001).

5.2. Late Weichselian glacial interval

Sea level progressively dropped in the eastern Mediterranean region during the transition to the last glacial maximum some 20 ka (e.g. Chappell

and Shackleton, 1986), reaching its lowest stand at −115 m in the Aegean Sea (Aksu et al., 1987), −100 m in the Marmara Sea (Smith et al., 1995; Aksu et al., 1999) and −110 m or deeper in the Black Sea (Ryan et al., 1997; Aksu et al., 2002). Because of sills in the Dardanelles (−78 m elevation at 20 ka) and Bosphorus (−40 m elevation), the Marmara Sea was completely isolated from both the Black Sea and the Aegean Sea during this time. The sedimentary record between ~21 and 15 ka is limited in our cores. However, seismic stratigraphic data show the presence of a number of stacked prograded delta successions along the shelf edge in the southern Marmara Sea. The most seaward foreset of the youngest delta was deposited immediately prior to the post-glacial sea-level rise at 11 ka (Aksu et al., 1999) when the rising Dardanelles sill was at ~−74 m elevation.

Palynological data from European lakes indicate that the climate in northern Europe immediately south of the ice margin was very cold and dry at ~20 ka; however, the Mediterranean climate was characterized by cold winters, intense winter precipitation, but summer droughts (Prentice et al., 1992; Peyron et al., 1998; Ramrath et al., 1999). Marine palynological data from the Marmara Sea also indicate relatively high winter precipitation during the Würm Pleniglacial and late Weichselian intervals (Mudie et al., 2002b). Limited data from the late glacial sediments in core MAR94-05 show that the fauna and flora in the Marmara Sea were marine during this time (Figs. 7 and 11), although the salinity was quite low (Fig. 15). Dinocyst assemblages indicate a surface-water salinity of 7–12‰ (Mudie et al., 2001).

5.3. Post-glacial interval

The global glacio-eustatic sea-level curve suggests that the post-glacial sea-level rise in the eastern Mediterranean started at ~14 ka (Chappell and Shackleton, 1986; Fairbanks, 1989). Between ~12 and 9.5 ka, the sea level rose from ~−77 m to ~−40 m. This time period was marked by the cessation of delta progradation along the shelf edge encircling the Aegean Sea (Aksu et al., 1987), as well as along the southern Marmara Sea shelf (Aksu et al., 1999) and the southwestern Black Sea shelf (Aksu et al., 2002). There was a rapid drowning and/or landward retreat of the deltas. The Straits of Bosphorus and Dardanelles (present-day depths of 40 and 70 m, respectively), and a sea level at −40 m allowed the initial connection between the Black Sea and the Aegean Sea via the Marmara Sea. However, the planktonic faunal, floral and stable isotopic data unequivocally show that the Marmara Sea surface waters were colder and of lower salinity during the transition from the late Weichselian to Holocene than today. Palynological data from the Black Sea and Marmara Sea cores also show that brackish to freshwater dinoflagellate cyst assemblages were present between ~12 and 9 ka (Mudie et al., 2001, 2002a). This is further corroborated by seismic stratigraphic and core data from the Black Sea, which show that sea level began to rise ~11 ka or earlier in the Black Sea, either in synchronity with or slightly ahead of the transgression in the Aegean Sea (Aksu et al., 2002). The youngest of two south-prograding deltas in the Marmara Sea at the southern entrance of the Strait of Bosphorus accumulated between 10 and 9 ka when the excess freshwater that had re-filled the Black Sea began flowing south, initially as a river crossing the modern Strait of Bosphorus (Hiscott et al., 2002). After ~9 ka, a salt wedge of Aegean Sea water penetrated sufficiently into the Bosphorus Strait to cut off bedload supply and terminate the construction of this delta lobe.

The transition from the late Weichselian glacial to the Holocene was characterized by a marked increase in precipitation across the entire Mediterranean region starting as early as 12 ka (Guiot et al., 1993; Harrison et al., 1993, 1996). Similar wetter conditions are also recorded in Europe about 1500 yr later. Increased pluviality over Europe is believed to have caused an increase in the discharge of rivers entering the Black Sea, so that it rapidly filled from its glacial maximum lowstand to the sill depth of the Strait of Bosphorus by ~10.5 ka (Aksu et al., 2002).

In the Marmara Sea, this interval of time is marked by the development of sapropel M1.

The ages of sapropels M1 in the Marmara Sea and S1 in the Aegean Sea are remarkably similar, occurring between ~10.5 and 6 ka in the Marmara Sea and 9.5 and 6.4 ka in the Aegean Sea (Aksu et al., 1995a,b; Çağatay et al., 1999, 2000; Görür et al., 2001). During this time, the surface-water circulation was dominated by southward export of Black Sea surface waters, with little northward penetration of Mediterranean surface water across the Bosphorus. The brackish water outflow since ~10.5 ka formed a low-salinity lid and enhanced vertical stratification, which prevented vertical mixing and caused very low oxygen concentrations to develop in the bottom waters of isolated basins.

At all studied core localities in the Marmara Sea (except at the shallowest core site MAR98-09), the onset of low-oxygen or suboxic conditions was rapid following the establishment of fully marine conditions at ~11 ka. As expected, there is a relationship between the BFOI values and water depth. The shallow sites, which are closer to the halocline at a modern depth of ~64 m (e.g. core MAR98-09) display slightly higher BFOI values than the two deeper sites. An unexpected finding is the noticeable upcore increase in BFOI values within the Holocene mud drape at all studied localities. This can be explained by increased ventilation of the sub-halocline waters during the later part of the Holocene. However, there is no evidence of a return to well-ventilated conditions at any time since the first connection to the Aegean Sea at ~11 ka. If the current estuarine-type circulation of the Marmara Sea had been disrupted by a rapid influx of well-oxygenated Mediterranean water at 7.1 ka (Ryan et al., 1997; Ryan and Pitman, 1999), the stable stratification of the water column would have broken down, leading to a well-oxygenated water column in which the planktonic foraminiferal, coccolith and dinoflagellate assemblages would have become dominated by typical Mediterranean fauna/flora, similar to those observed in the Aegean Sea cores (e.g. Aksu et al., 1995b). The micropaleontological evidence does not support such a scenario. The absence of subtropical Mediterranean fauna and flora in any significant numbers in Marmara Sea cores and the overwhelming dominance of subpolar–transitional species, often endemic to lower salinity water masses, do not permit the presence of a Mediterranean surface-water mass in the Marmara Sea during this time. Instead, the slight but gradual increase in BFOI values probably reflects a decreasing volume of Black Sea outflow through time and a weakening of the halocline, promoting slightly better ventilation of the Marmara Sea deep water.

6. Conclusions

During the last ~30 000 yr, the Marmara Sea was isolated from both the Black Sea and the Aegean Sea during glacial periods when low global sea level subaerially exposed the shallow sills at the Straits of Bosphorus and Dardanelles (i.e. lake stage). The three water bodies were reconnected during interglacial periods, when rising global sea level breached the shallow sills in the straits (i.e. gateway stage). The salient conclusions of our core studies are:

(1) Two sapropel layers are present in the Marmara Sea cores: sapropels M2 and M1 were deposited between ~29.5 and 23.5 ka, and ~10.5 and 6 ka, respectively. Stable isotopic and micropaleontological data show that the surface-water salinities were reduced considerably during the deposition of both sapropels. A planktonic foraminiferal transfer function shows that SSTs were notably lower during these intervals. The absence of Mediterranean fauna and flora in sapropels M1 and M2 strongly suggests that communication existed with the Black Sea during these times, with colder and lower salinity waters flowing into the Mediterranean Sea via the Straits of Bosphorus and Dardanelles and the Marmara Sea.

(2) Sapropel layer M1 developed mainly as the result of intensified water-mass stratification in the Marmara Sea, as the lower salinity, cooler Black Sea surface waters extended across the Marmara Sea. The paucity of benthic foraminifera, and the rare and sporadic occurrences of dysoxic species suggest that deep-water conditions during the deposition of sapropel M1 must have been close to anoxic. Near the top of the sapropel

layer, a bloom in *Globobulimina* indicates slight improvement in the bottom-water oxygenation.

(3) The multi-proxy core data do not support the Ryan et al. (1997) and Ryan and Pitman (1999) hypothesis that at ~7.1 ka the level of the Marmara Sea rose to breach the Strait of Bosphorus and initiate a cascade into the Black Sea. Instead, the data show that at ~10.5 ka the Black Sea rose to the breach depth of the Bosphorus and flowed into the Marmara Sea, developing a cooler, low-salinity surface layer, and promoting the deposition of sapropel M1 in the Marmara Sea, and sapropel S1 in the Aegean Sea.

Acknowledgements

We thank Prof. Dr. Erol Izdar, the Director of the Piri Reis Foundation for Maritime and Marine Resources Development and Education, and Prof. Dr. Orhan Uslu, the Director of the Institute of Marine Sciences and Technology, for their support and encouragement. We extend our special thanks to the officers and crew of the RV *Koca Piri Reis* for their assistance in data acquisition, in particular Captain Mehmet Özsaygılı and Chief Engineer Ömer Çubuk. We acknowledge the assistance of Alison Pye in stable isotopic analyses. We acknowledge research funds from the Natural Sciences and Engineering Research Council of Canada (NSERC) to A.E.A. and R.N.H., ship-time funds from NSERC to A.E.A. and R.N.H., travel funds from the Dean of Science at MUN, and special grants from the Piri Reis Foundation for Maritime and Marine Resources Development and Education, Turkey. Simone Galeotti and Kay-Christian Emeis critically read the manuscript and provided many valuable comments.

References

Abrajano, T., Aksu, A.E., Hiscott, R.N., Mudie, P.J., 2002. Aspects of carbon isotope biogeochemistry of late Quaternary sediments from the Marmara Sea and Black Sea. Mar. Geol. 190, S0025-3227(02)00346-8.

Aksu, A.E., Piper, D.J.W., Konuk, T., 1987. Late Quaternary tectonic and sedimentation history of Outer Izmir Bay and Çandarlı Basin, Western Turkey. Mar. Geol. 76, 89–104.

Aksu, A.E., de Vernal, A., Mudie, P.J., 1989. High resolution foraminifer, palynologic and stable isotopic records of Upper Pleistocene sediments from the Labrador Sea: Paleoclimatic and paleoceanographic trends. In: Srivastava, S.P., Arthur, M., Clement, B. et al. (Eds.), Proc. ODP Sci. Results, 105, pp. 617–652.

Aksu, A.E., Yaşar, D., Mudie, P.J., 1995a. Paleoclimatic and paleoceanographic conditions leading to development of sapropel layer S1 in the Aegean Sea basins. Palaeoclimatol. Palaeogeogr. Palaeoecol. 116, 71–101.

Aksu, A.E., Yaşar, D., Mudie, P.J., Gillespie, H., 1995b. Late glacial–Holocene paleoclimatic and paleoceanographic evolution of the Aegean Sea: micropaleontological and stable isotopic evidence. Mar. Micropaleontol. 25, 1–28.

Aksu, A.E., Hiscott, R.N., Yaşar, D., 1999. Oscillating Quaternary water levels of the Marmara Sea and vigorous outflow into the Aegean Sea from the Marmara Sea-Black Sea drainage corridor. Mar. Geol. 153, 275–302.

Aksu, A.E., Hiscott, R.N., Yaşar, D., Işler, F.I., Marsh, S., 2002. Seismic stratigraphy of Late Quaternary deposits from the southwestern Black Sea shelf: evidence for non-catastrophic variations in sea-level during the last ~10 000 years. Mar. Geol. 190, S0025-3227(02)00343-2.

Almogi-Labin, A., Luz, B., Duplessy, J.C., 1986. Quaternary paleo-oceanography, pteropod preservation and stable isotopic record of the Red Sea. Palaeogeogr. Palaeoclimatol. Palaeoecol. 57, 195–211.

Berger, W.H., 1977. Deep-sea carbonate and the deglaciation preservation spike in pteropods and foraminifera. Nature 269, 301–304.

Bernhard, J.M., 1986. Characteristic assemblages and morphologies of benthic foraminifera from anoxic, organic-rich deposits: Jurassic through Holocene. J. Foraminifer. Res. 16, 207–215.

Beşiktepe, Ş., Sur, H.I., Özsoy, E., Latif, M.A., Oğuz, T., Ünlüata, Ü., 1994. The circulation and hydrography of the Marmara Sea. Prog. Oceanogr. 34, 285–334.

Bukry, D., 1974. Coccoliths as paleosalinity indicators – evidence from Black Sea. In: Degens, E.T., Ross, D.A. (Eds.), The Black Sea – Geology, Chemistry and Biology. American Association of Petroleum Geologists, Memoir 20, pp. 352–363.

Çağatay, N.M.O., Sakınç, M., Eastoe, C., Egesel, L., Balkıs, N., Ongan, D., Caner, H., 1999. A mid-late Holocene sapropelic sediment unit from the southern Marmara shelf and its paleoceanographic significance. Quat. Sci. Rev. 18, 531–540.

Çağatay, N.M.O., Görür, N., Algan, O., Eastoe, C., Tchapalyga, A., Ongan, D., Kuhn, T., Kuşçu, I., 2000. Late glacial–Holocene paleoceanography of the Sea of Marmara: timing of connections with the Mediterranean and the Black Seas. Mar. Geol. 167, 191–206.

Castradori, D., 1993. Calcareous nannofossil biostratigraphy and biochronology in eastern Mediterranean deep-sea cores. Riv. Ital. Paleontol. Stratigr. 99, 107–126.

Chappell, J., Shackleton, N.J., 1986. Oxygen isotopes and sea level. Nature 324, 137–140.

Corliss, B.H., Chen, C., 1988. Morphotype patterns of Norwegian Sea deep-sea benthic foraminifera and ecological implications. Geology 16, 716–719.

Erba, E., Parisi, E., Cita, M.B., 1987. Stratigraphy and sedimentation in the western Strabo Trench, Eastern Mediterranean. Mar. Geol. 75, 57–75.

Fairbanks, R.G., 1989. A 17 000-year glacio-eustatic sea level record: influence of glacial melting rates on the Younger Dryas event and deep-ocean circulation. Nature 342, 637–642.

Görür, N., Çağatay, M.N., Emre, Ö., Alpar, B., Sakınç, M., Islamoğlu, Y., Algan, O., Erkal, T., Keçer, M., Akkök, R., Karlık, G., 2001. Is the abrupt drowning of the Black Sea shelf at 7150 yr BP a myth? Mar. Geol. 176, 65–73.

Guiot, J., Harrison, S., Prentice, I.C., 1993. Reconstruction of Holocene precipitation patterns in Europe using pollen and lake-level data. Quat. Res. 40, 139–149.

Harrison, S.P., Prentice, I.C., Guiot, J., 1993. Climatic controls of Holocene lake-level changes in Europe. Clim. Dyn. 8, 189–200.

Harrison, S.P., Yu, G., Tarasov, P., 1996. Late Quaternary lake-level record from northern Eurasia. Quat. Res. 45, 138–159.

Hiscott, R.N., Aksu, A.E., 2002. Late Quaternary history of the Marmara Sea and Black Sea from high-resolution seismic and gravity-core studies. Mar. Geol. 190, S0025-3227(02)00350-x.

Hiscott, R.N., Aksu, A.E., Yaşar, D., Kaminski, M.A., Mudie, P.J., Kostylev, V., MacDonald, J., Işler, F.I., Lord, A.R., 2002. Deltas south of the Bosphorus Strait record persistent Black Sea outflow to the Marmara Sea since ~10 ka. Mar. Geol. 190, S0025-3227(02)00344-4.

Huijzer, B., Vandenberghe, J., 1998. Climatic reconstruction of the Weichselian Pleniglacial in northwestern and central Europe. J. Quat. Sci. 13, 391–417.

Imbrie, J., Hays, J.D., Martinson, D.G., McIntyre, A., Mix, A.C., Morley, J.J., Pisias, N.G., Prell, W.L., Shackleton, N.J., 1984. The orbital theory of Pleistocene climate: support from revised chronology of the marine $\delta^{18}O$ record. In: Berger, A.L., Imbrie, J., Hays, J., Kukla, G., Saltzman, B. (Eds.), Milankovitch and Climate, Part I, NATO ASI Series C, Vol. 126. D. Reidel Publishing Company, Dordrecht, pp. 269–305.

Kaiho, K., 1991. Global changes of Paleogene aerobic–bic benthic foraminifera and deep sea circulation. Palaeogeogr. Palaeoclimatol. alaeoecol. 83, 65–85.

Kaiho, K., 1994. Benthic foraminiferal dissolved-oxygen index and dissolved-oxygen levels in the modern ocean. Geology 22, 719–722.

Kaminski, M.A., Aksu, A.E., Box, M., Hiscott, R.N., Filipescu, S., Al-Salameen, M., 2002. Late glacial to Holocene benthic foraminifera in the Marmara Sea: implications for Black Sea – Mediterranean Sea connections following the last deglaciation. Mar. Geol. 190, S0025-3227(02)00347-x.

Kennett, J.P., Srinivasan, M.S., 1983. Neogene Planktonic Foraminifera: A Phylogenetic Atlas. Hutchinson Ross Publishing Company, Stroudsburg, PA, 265 pp.

Kidd, R.B., Cita, M.B., Ryan, W.B.F., 1978. Stratigraphy of eastern Mediterranean sapropel sequences recovered during DSDP Leg 42A and their paleoenvironmental significance. In: Hsü, K.J., Montadert, L. et al. (Eds.), Initial Reports of the Deep Sea Drilling Project, Volume 42, Part 1. U.S. Government Printing Office, Washington, DC, pp. 421–443.

Kleijne, A., 1993. Morphology, Taxonomy and Distribution of Extant Coccolithophorids (Calcareous Nannoplankton). Drukkerij FEBA B.V., Enschede, 321 pp.

Knappertsbusch, M., 1993. Geographic distribution of living and Holocene coccolithophores in the Mediterranean Sea. Mar. Micropaleontol. 21, 219–247.

Latif, M.L., Özsoy, E., Salihoğlu, I, Gaines, A.F., Baştürk, Ö., Yılmaz, A., Tuğrul, S., 1992. Monitoring via Direct Measurements of the Modes of Mixing and Transport of Wastewater Discharges into the Bosphorus Underflow. Middle East Technical University, Institute of Marine Sciences, Technical Report No. 92-2, 98 pp.

MacDonald, J., 2000. Molluscs and Bivalves in Cores from the Marmara Sea and Black Sea. Unpublished B.Sc. thesis, Memorial University of Newfoundland, 90 pp.

Mestel, R., 1997. Noah's flood. New Sci. 156, 24–27.

Mudie, P.J., Aksu, A.E., Yaşar, D., 2001. Late Quaternary dinocysts from the Black, Marmara and Aegean Seas: variations in assemblages, morphology and paleosalinity. Mar. Micropaleontol. 43, 155–178.

Mudie, P.J., Rochon, A., Aksu, A.E., Gillespie, H., 2002. Dinoflagellate cysts, freshwater algae and fungal spores as salinity indicators in Late Quaternary cores from Marmara and Black Seas. Mar. Geol. 190, S0025-3227(02)00348-1.

Mudie, P.J., Rochon, A., Aksu, A.E., 2002. Pollen stratigraphy of Late Quaternary cores from Marmara Sea: land-sea correlation and paleoclimatic history. Mar. Geol. 190, S0025-3227(02)00349-3.

Oğuz, T., Latun, V.S., Latif, M.A., Vladimirov, V.V., Sur, H.I., Markov, A.A., Özsoy, E., Kotovshchikov, B.B., Eremeev, V.V., Ünlüata, Ü., 1993. Circulation in the surface and intermediate layers of the Black Sea. Deep-Sea Res. I 40, 1597–1612.

Olausson, E., 1961. Studies of deep sea cores. Rep. Swed. Deep-Sea Exped. 1947–1948 8, 323–438.

Özsoy, E., Latif, M.A., Tuğrul, S., Ünlüata, Ü., 1995. Exchanges with the Mediterranean, fluxes and boundary mixing processes in the Black Sea. In: Briand, F. (Ed.), Mediterranean Tributary Seas. Bulletin de l'Institut Océanographique, Monaco, Special No. 15, CIESME Science Series 1, pp. 1–25.

Özsoy, E., Latif, M.A., Sur, H.I., Goryachkin, Y., 1996. A review of the exchange flow regimes and mixing in the Bosphorus Strait. In: Briand, F. (Ed.), Mediterranean Tributary Seas. Bulletin de l'Institut Océanographique, Monaco, Special No. 17, CIESME Science Series 2, pp. 187–204.

Peyron, O., Guiot, J., Cheddadi, R., Tarasov, P., Reille, M., de Beaulieu, J.-L., Bottema, S., Andrieu, V., 1998. Climatic

reconstruction in Europe for 18 000 yr BP from pollen data. Quat. Res. 49, 183–196.

Polat, Ç., Tuğrul, S., 1996. Chemical exchange between the Mediterranean and Black Sea via the Turkish Straits. In: Briand, F. (Ed.), Dynamics of Mediterranean Straits and Channels. Bulletin de l'Institut Océanographique, Monaco, Special No. 17, CIESME Science Series 2, pp. 167–186.

Prentice, I.C., Guiot, J., Harrison, S.P., 1992. Mediterranean vegetation, lake-level and paleoclimate at the Last Glacial Maximum. Nature 360, 658–670.

Raffi, I., Backman, J., Rio, D., Shackleton, N.J., 1993. Plio-Pleistocene nannofossil biostratigraphy and calibration to oxygen isotope stratigraphies from Deep Sea Drilling Project Site 607 and Ocean Drilling Program Site 677. Paleoceanography 8, 387–408.

Ramrath, A., Zolitschka, B., Wulf, S., Negendank, J.F.W., 1999. Late Pleistocene climatic variations as recorded in two Italian maar lakes (Lago di Mezzano, Lago Grande di Monticchio). Quat. Sci. Rev. 18, 977–992.

Rank, D., Özsoy, E., Salihoğlu, I., 1999. Oxygen-18, deuterium and tritium in the Black Sea and the Sea of Marmara. J. Environ. Radioact. 43, 231–245.

Roberts, N., 1983. Age, paleoenvironments and climatic significance of Late Pleistocene Konya Lake, Turkey. Quat. Res. 19, 154–171.

Rossignol-Strick, M., 1985. Mediterranean Quaternary sapropels, an immediate response of the African monsoon to variation of insolation. Palaeogeogr. Palaeoclimatol. Palaeoecol. 49, 237–263.

Ryan, W.B.F., Pitman, W.C., III, Major, C.O., Shimkus, K., Maskalenko, V., Jones, G.A., Dimitrov, P., Görür, N., Sakinç, M., Yüce, H., 1997. An abrupt drowning of the Black Sea shelf. Mar. Geol. 138, 119–126.

Ryan, W.B.F., Pitman III, W.C., 1999. Noah's Flood: the New Scientific Discoveries about Events that Changed History. Simon and Schuster, New York, 319 pp.

Saito, T., Thompson, P.R., Breger, D., 1981. Systematic Index of Recent and Pleistocene Planktonic Foraminifera. University of Tokyo Press, 190 pp.

Shackleton, N.J., 1974. Attainment of isotopic equilibrium between ocean water and benthonic foraminifera genus *Uvigerina*: isotopic changes in the ocean during the last glacial. Cent. Natl. Rech. Sci. Colloq. Int. 219, 203–209.

Skene, K.I., Piper, D.J.W., Aksu, A.E., Syvitski, J.M.P., 1998. Evaluation of the global oxygen isotope curve as a proxy for Quaternary sea level by modelling of delta progradation. J. Sediment. Res. 68, 1077–1092.

Smith, A.D., Taymaz, T., Oktay, F., Yüce, H., Alpar, B., Başaran, H., Jackson, J.A., Kara, S., Şimşek, M., 1995. High-resolution seismic profiling in the Sea of Marmara (northwest Turkey): Late Quaternary sedimentation and sea-level changes. Geol. Soc. Am. Bull. 107, 923–936.

Stuiver, M., Reimer, P.J., Bard, E., Beck, J.W., Burr, G.S., Hughen, K.A., Kromer, B., McCormac, G., van der Plicht, J., Spurk, M., 1998a. INTCAL98 radiocarbon age calibration, 24000–0 cal BP. Radiocarbon 40, 1041–1083.

Stuiver, M., Reimer, P.J., Braziunas, T.F., 1998b. High-precision radiocarbon age calibration for terrestrial and marine samples. Radiocarbon 40, 1127–1151.

Thunell, R.C., 1978. Distribution of recent planktonic foraminifera in surface sediments of the Mediterranean Sea. Mar. Micropaleontol. 3, 147–173.

Thunell, R.C., 1979. Eastern Mediterranean Sea during the last glacial maximum; an 18 000-years B.P. reconstruction. Quat. Res. 11, 353–372.

Thunell, R.C., Williams, D.F., 1989. Glacial–Holocene salinity change in the Mediterranean Sea: hydrographic and depositional effects. Nature 338, 493–496.

UNESCO, 1969. Discharge of Selected Rivers of the World, Vol. 1: General and Regime Characteristics of Stations Selected. Studies and Reports in Hydrology, 70 pp.

UNESCO, 1993. Discharge of Selected Rivers of the World. Monthly and Annual Discharges Recorded at Various Selected Stations. Studies and Reports in Hydrology, V2, 600 pp.

Vergnaud-Grazzini, C., Ryan, W.B.F., Cita, M.B., 1977. Stable isotope fractionation, climate change and episodic stagnation in the eastern Mediterranean during the Late Quaternary. Mar. Micropaleontol. 2, 353–370.

Volkman, R., Mensch, M., 2001. Stable isotopic composition of living planktonic foraminifers in the outer Leptev Sea and Fram Strait. Mar. Micropaleontol. 42, 163–188.

Winter, A., Jordan, R.W., Roth, P.H., 1994. Biogeography of the living coccolithophores in the oceans. In: Winter, A., Siesser, W. (Eds.), Coccolithophores. Cambridge University Press, Cambridge, pp. 161–178.

Yaltırak, C., Sakınç, M., Aksu, A.E., Galleb, B, Hiscott, R.N., Ülgen, U.G., 2002. Late Pleistocene uplift history along the southwestern Marmara Sea determined from raised coastal deposits and global sea-level variations. Mar. Geol. 190, S0025-3227(02)00351-1.